

# Software News and Updates

## The MP2-F12 Method in the TURBOMOLE Program Package

RAFAŁ A. BACHORZ,<sup>1</sup> FLORIAN A. BISCHOFF,<sup>2</sup> ANDREAS GLÖB,<sup>3</sup> CHRISTOF HÄTTIG,<sup>4</sup> SEBASTIAN HÖFENER,<sup>1\*</sup>  
WIM KLOPPER,<sup>1</sup> DAVID P. TEW<sup>5</sup>

<sup>1</sup>Center for Functional Nanostructures (CFN) and Institute of Physical Chemistry,  
Karlsruhe Institute of Technology, KIT Campus South, P.O. Box 6980, D-76049 Karlsruhe, Germany

<sup>2</sup>Department of Chemistry, Virginia Tech, 107 Davidson Hall, Blacksburg, Virginia 24061

<sup>3</sup>Laboratory of Physical Chemistry, ETH Hönggerberg, HCI, CH-8093 Zurich, Switzerland

<sup>4</sup>Lehrstuhl für Theoretische Chemie, Ruhr-Universität Bochum, D-44780 Bochum, Germany

<sup>5</sup>School of Chemistry, University of Bristol, Bristol BS8 ITS, United Kingdom

Received 29 November 2010; Revised 25 March 2011; Accepted 27 March 2011

DOI 10.1002/jcc.21825

Published online 17 May 2011 in Wiley Online Library (wileyonlinelibrary.com).

**Abstract:** A detailed description of the explicitly correlated second-order Møller–Plesset perturbation theory (MP2-F12) method, as implemented in the TURBOMOLE program package, is presented. The TURBOMOLE implementation makes use of density fitting, which greatly reduces the prefactor for integral evaluation. Methods are available for the treatment of ground states of open- and closed-shell species, using unrestricted as well as restricted (open-shell) Hartree–Fock reference determinants. Various methodological choices and approximations are discussed. The performance of the TURBOMOLE implementation is illustrated by example calculations of the molecules leflunomide, prednisone, methotrexate, ethylenedioxytetrafulvalene, and a cluster model for the adsorption of methanol on the zeolite H-ZSM-5. Various basis sets are used, including the correlation-consistent basis sets specially optimized for explicitly correlated calculations (cc-pVXZ-F12).

© 2011 Wiley Periodicals, Inc. J Comput Chem 32: 2492–2513, 2011

**Key words:** Turbomole program; MP2-F12 method; explicit correlation; perturbation theory; density fitting

### Introduction

F12 explicitly correlated methodologies have now entered mainstream electronic structure theory as a direct and efficient solution to the basis set problem for dynamic correlation. F12 techniques have been combined predominantly with pair theories, such as second-order Møller–Plesset perturbation theory (MP2) and coupled cluster singles-and-doubles (CCSD) theory, and basis set limit energies are routinely obtained with these F12 methods using only medium-sized orbital basis sets.<sup>1–3</sup> Although historically the field of R12/F12 explicit correlation has been associated with an abundance of approximations and associated acronyms, this has now crystallized to a few useful variants through a consensus among the community of developers. Furthermore, specially optimized orbital and auxiliary basis sets are now available for F12 methods,<sup>4–8</sup> and the calculations can be performed in a black-box manner, at least for compounds of light elements. The double-zeta F12 basis sets are sufficient to reduce the basis set incompleteness errors of F12 methods to below 0.30 kJ/mol per valence electron for reaction energies while basis set errors with triple-zeta F12 basis sets are less than 0.05 kJ/mol per valence electron, which can be further reduced through extrapolation.<sup>9</sup>

The aim for computation in electronic structure theory is ultimately to provide reliably accurate or quantitative chemical predictions.<sup>10,11</sup> In many cases, this means accounting for three-electron and even higher order correlation effects. In this context, MP2-F12 and CCSD-F12 methods are useful for eliminating basis set errors in the dominant pair interactions and providing estimates for the basis

Additional Supporting Information may be found in the online version of this article.

**Correspondence to:** W. Klopper: e-mail: klopper@kit.edu

Contract/grant sponsor: Deutsche Forschungsgemeinschaft [Center for Functional Nanostructures (CFN)]; contract/grant number: C3.3

Contract/grant sponsor: Ministry of Science, Research and the Arts of Baden-Württemberg; contract/grant number: Az: 7713.14-300

Contract/grant sponsors: Fonds der chemischen Industrie, German Academic Exchange Service (DAAD), Deutsche Telekom Stiftung, European Commission [Marie Curie Intra-European Fellowship (IEF) scheme], Royal Society (University Research Fellowship scheme).

\*Present address: Amsterdam Center for Multiscale Modeling, Division of Theoretical Chemistry, VU University Amsterdam, De Boelelaan 1083, NL-1081 HV Amsterdam, The Netherlands.

set error in the higher order corrections. This article is concerned exclusively with MP2-F12 theory, which is a prerequisite for CCSD-F12 and CCSD(T)-F12 methods (see, for example, Ref. 12). The MP2-F12 method is also useful in its own right as a tool for the computational treatment of weak interactions between large systems, in particular for hydrogen-bonded systems. For typical van der Waals systems, the method may be applied in its spin-component-scaled (SCS) variant.<sup>13,14</sup> Conventional CCSD and CCSD(T) calculations may be augmented with corrections obtained from MP2-F12 theory, as for example recently done in large-scale calculations on a trimer of pyrazine,<sup>15</sup> and the basis set error of a given basis may be estimated from MP2-F12 calculations, noting that the basis set errors at higher levels are usually smaller than at the MP2 level.<sup>16,17</sup>

The aim of this article is to present the details of the MP2-F12 method for ground state energies, to present its implementation in the TURBOMOLE program and to demonstrate the range of utility currently affordable. For this purpose and as a reference for future work, we briefly review the theory, although no new aspects are added. Not only the MP2-F12 method but also the SCS-MP2-F12 method is available in the TURBOMOLE program package.<sup>14</sup>

The calculations presented in this article were performed with version 6.3 of the TURBOMOLE program package<sup>18</sup> (A development of Universität Karlsruhe (TH) and Forschungszentrum Karlsruhe GmbH, 1989–2007, TURBOMOLE GmbH, since 2007. The TURBOMOLE program package can be obtained from redistributor COSMOlogic GmbH & Co. KG in Leverkusen, Germany. For information on license schemes, prices, how to order the TURBOMOLE program package, please contact COSMOlogic GmbH & Co. KG via turbomole@cosmologic.de.).

### General Philosophy

The TURBOMOLE program package aims at application to large systems using desktop machines, thus efficient procedures are adopted, and the routines are designed with low disk and memory requirements.<sup>19</sup> The MP2-F12 implementation is therefore in line with these design principles, making calculations on sizable systems feasible. Standard MP2 (and CC2) calculations can be performed using the RICC2 module of the TURBOMOLE suite, which is applicable to systems as large as compounds of the composition C<sub>5</sub>H<sub>61</sub>O<sub>59</sub>Si<sub>37</sub>Al, even in a TZVP basis.<sup>20</sup> The salient features of the MP2 and CC2 implementations are the use of density fitting, which greatly reduces the prefactor for integral evaluation, and that storage of four-index quantities is avoided, which ensures low disk usage. The MP2-F12 method has been implemented in the RICC2 module and adopts these efficient techniques and uses many of the same routines. Density fitting is used for all two-electron integral evaluations, and four-index integrals are evaluated at the point they are required and are not stored on disk.

Regarding the various methodological choices within F12 theory, the approximations that are implemented are consistent and conservative, preserving the accuracy of the approach. The methods available are those that give a balanced description of open- and closed-shell species and preference is given to the variants with the lowest scaling with system size.

Our implementation takes care of the general applicability of the code, that is, by allowing to use effective core potentials

(ECPs<sup>21</sup>) and/or finite external fields and point charges for (periodic) electrostatic embedding purposes.<sup>22</sup>

### F12 Basis Functions

In standard Møller–Plesset and coupled cluster methods, the wave function is expressed as a linear combination of the Hartree–Fock (HF) wave function and excited configurations. Two-body electron–electron interactions are accounted for through double excitations, where a pair of occupied spin orbitals  $|ij\rangle$  is replaced by a linear combination of pair functions  $|ab\rangle$ , where  $a, b$  are virtual spin orbitals. The essence of F12 theory is to use a basis of pair functions  $|w_{xy}\rangle$  in addition to the standard pair basis  $|ab\rangle$ , where  $|w_{xy}\rangle$  depends explicitly on  $r_{12}$ , the distance between two electrons. The level of correlation treatment is unchanged, while the basis set limit for the parameterization of the double excitations is approached more rapidly than for standard methods. The reason that F12 methods achieve near basis set limit accuracy with relatively small basis sets is because the F12 basis functions efficiently describe the sharp features of the wave function in the region of short-range  $r_{12}$ , that is, the correlation cusp. In this way, the  $X^{-3}$  energy convergence of the orbital expansion is accelerated to  $X^{-7}$  for F12 methods, where  $X$  is the cardinal number of the orbital basis set.

The F12 basis functions are given by

$$|w_{xy}\rangle = \hat{Q}_{12}f_{12}\hat{S}_{xy}|xy\rangle. \quad (1)$$

The spin orbitals  $x, y$  are chosen to be the active occupied orbitals.  $f_{12}$  is the correlation factor, which has a length scale parameter  $\gamma$ :

$$f_{12} = \sum_{v=1}^n c_v e^{-\gamma v r_{12}^2} \approx (-1/\gamma)e^{-\gamma r_{12}^2}. \quad (2)$$

Between 3 and 6 Gaussian functions can be used to fit the Slater-type correlation factor. The exponents and coefficients are taken from Ref. 23 for  $\gamma = 1 a_0^{-1}$  and scaled appropriately.  $\hat{Q}_{12}$  is the strong orthogonality operator, which ensures that the F12 basis functions are strongly orthogonal to the Hartree–Fock reference and orthogonal to the conventional double excitations:

$$\hat{Q}_{12} = (1 - \hat{O}_1)(1 - \hat{O}_2) - \hat{V}_1\hat{V}_2, \quad (3)$$

where  $\hat{O}$  and  $\hat{V}$  project onto the space of occupied (active and frozen) and active virtual spin orbitals, respectively:

$$\hat{O} = \sum_o |o\rangle\langle o|, \quad (4)$$

$$\hat{V} = \sum_a |a\rangle\langle a|. \quad (5)$$

The rational generator  $\hat{S}_{xy}$  ensures that the  $s$ - and  $p$ -wave coalescence conditions are satisfied for both restricted and unrestricted first-order wave functions:

$$\hat{S}_{xy} = \frac{3}{8} + \frac{1}{8}\hat{P}_{xy}, \quad (6)$$

$$\hat{P}_{xy}\varphi_x(1)\sigma_x(1)\varphi_y(2)\sigma_y(2) = \varphi_y(1)\sigma_x(1)\varphi_x(2)\sigma_y(2), \quad (7)$$

where  $\varphi_x$  and  $\sigma_x$  are the space and spin components of spin orbital  $\phi_x$ , respectively.

As the F12 geminal basis functions efficiently parametrize the space of double excitations and effectively eliminate this source of basis set error, the basis set error in the HF energy becomes important. This is particularly true for calculations with double- or triple-zeta orbital basis sets. Therefore, F12 methods also include a perturbative correction for the HF basis set error<sup>24,25</sup> by including single excitations from the occupied Hartree–Fock orbitals to the complementary auxiliary basis set. Doing so, both the Hartree–Fock part and the correlation contribution exhibit comparable error bars such that neither one is the bottleneck in terms of accuracy.

### Notation and Definitions

For reasons of continuity with a forthcoming article on CCSD-F12 theory, we present equations using the formalism of second quantization. We will use the short hands  $a_q^p = a^p a_q$ , and  $a_{qs}^{pr} = a^p a^r a_s a_q$ , where  $a^p$  and  $a_q$  are normal-ordered creation and annihilation operators, respectively.  $p, q, \dots$  are the spin orbitals of the occupation number representation. The Hamiltonian is written as

$$\hat{H} = E^0 + \hat{F} + \hat{G}, \quad (8)$$

where  $E^0 = \langle 0 | \hat{H} | 0 \rangle$  is the energy of the reference determinant  $|0\rangle$ . The Fock operator  $\hat{F}$  is given by

$$\hat{F} = f_p^q a_p^q. \quad (9)$$

We use the Einstein summation convention, where a summation over repeated indices is implied. The Fock operator decomposes into contributions

$$\hat{F} = \hat{T} + \hat{V} + \hat{J} - \hat{K} + \hat{U}, \quad (10)$$

$$f_p^q = h_p^q + j_p^q - k_p^q + u_p^q. \quad (11)$$

$\hat{T} + \hat{V}$  is the core Hamiltonian,  $\hat{J}$  and  $\hat{K}$  are the Coulomb and exchange operators, respectively, and  $\hat{U}$  contains all other non-multiplicative operators, such as an effective core potential, or the mass-velocity operator. Multiplicative operators such as electric fields are included in  $\hat{V}$ . The fluctuation potential  $\hat{G}$  is given by

$$\hat{G} = g_{pr}^{qs} a_{qs}^{pr}, \quad (12)$$

where  $g_{pr}^{qs} = \langle pr | r_{12}^{-1} | qs \rangle$  are antisymmetrized two-electron repulsion integrals in the (12|12) notation. For the pair indices, we adopt the convention that  $p < r$  and  $q < s$ .

We will use  $|p\rangle = \phi_p$  to denote a spin orbital with spatial and spin components  $\varphi_p \sigma_p$ .  $|pq\rangle$  always refers to a Slater determinant

$$|pq\rangle = (\phi_p \phi_q - \phi_q \phi_p) / \sqrt{2}, \quad (13)$$

whereas  $|\phi_p \phi_q\rangle = \phi_p \phi_q$ , thus

$$\langle pr | r_{12}^{-1} | qs \rangle = \langle \phi_p \phi_r | r_{12}^{-1} | \phi_q \phi_s \rangle - \langle \phi_p \phi_r | r_{12}^{-1} | \phi_s \phi_q \rangle. \quad (14)$$

**Table 1.** A summary of index conventions.

$p, q, r, \dots$	Orbitals in the HF basis
$i, j, k, \dots$	Active occupied orbitals
$o$	Active and frozen occupied orbitals
$a, b, c, \dots$	Active virtual orbitals in the finite basis
$\alpha, \beta, \gamma, \dots$	Virtual orbitals in a formally complete basis
$\alpha', \beta', \gamma', \dots$	Complementary virtual orbitals in a formally complete basis
$a', b', c', \dots$	CABS representation of complementary virtual orbitals
$p', q', r', \dots$	Orbitals in the HF plus CABS basis
$v, w, x, \dots$	Orbitals of the F12 geminal basis
$\kappa, \lambda, \mu, \dots$	Atomic orbitals in finite basis
$\kappa', \lambda', \mu', \dots$	CABS atomic orbitals
$P, Q, R, \dots$	Auxiliary basis set for density fitting

Furthermore, we will use the notation

$$(pq | r_{12}^{-1} | rs) \quad (15)$$

to denote integrals over spatial orbitals  $\varphi_p(1)$ ,  $\varphi_q(1)$ ,  $\varphi_r(2)$ , and  $\varphi_s(2)$ .

To represent the F12 geminal basis functions using second quantization (see next section), it is necessary to introduce a formally complete set of orbitals. All of the definitions above apply transparently to such a basis, because one only has to extend  $a, b, \dots$ ,  $p, q, \dots$  to run over the orbitals of the complete basis. The formally complete orbital space can be partitioned into the orbitals occupied in the HF reference  $i$ , and a formally complete set of virtuals  $\alpha$ . In turn, this space of virtual orbitals can be partitioned into orbitals  $a$ , the virtuals spanned by the finite orbital basis (used to determine the Fock operator and the HF reference determinant) and the rest  $\alpha'$ . Certain aspects of F12 theory, connected to the RI insertion used to approximate three-electron integrals in terms of two-electron integrals, require a programmable representation of the complementary virtuals  $\alpha'$ . For this, a complementary auxiliary basis (CABS) is used to define a set of virtual orbitals  $a'$  that are a subset of  $\alpha'$ . This set is constructed by orthogonalizing the CABS functions against the HF basis. A summary of the indices and the spaces they refer to are given in Table 1.

Concerning the Fock matrix  $f$ , for a determinant from a RHF or UHF calculation in the orbital basis, the condition that matrix elements  $f_i^a = 0$  is known as the Brillouin condition. The matrix elements  $f_i^{\alpha'}$  and  $f_a^{\alpha'}$  on the other hand are not in general zero. For a reasonable orbital basis, the elements  $f_i^{\alpha'}$  are expected to be small. Assuming that they are zero is referred to as (assuming) the generalized Brillouin condition (GBC). For an almost complete orbital basis, the elements  $f_a^{\alpha'}$  will also be small and are taken to be zero if the extended Brillouin condition (EBC) is assumed.

## Theory

### The Zeroth- and First-Order Wave functions

The chosen partitioning of the Hamiltonian into a zeroth-order operator and a perturbation is

$$\hat{H} = E^0 + \hat{F}^0 + \hat{F}^1 + \hat{G}^1. \quad (16)$$

$\hat{G}^1 = \hat{G}$  and  $\hat{F}^0 = \hat{F} - \hat{F}^1$ , where

$$\hat{F}^1 = f_{\alpha}^i a_i^{\alpha} + f_i^{\alpha} a_{\alpha}^i. \quad (17)$$

Thus, the HF wave function  $|0\rangle$  in the finite orbital basis is a true eigenfunction of the zeroth-order operator for restricted (RHF), unrestricted (UHF), and restricted open-shell (ROHF) wave functions. Note that  $|0\rangle$  is not in general a true eigenfunction of  $\hat{F}$  even for RHF cases, because they both result from a HF calculation in a finite orbital basis—in other words, the occupied orbitals are in practice never fully converged to the basis set limit. To first order, both single and double excitations enter the wave function. In F12 theory, the first-order wave function is expanded as

$$|1\rangle = (T_1 + T_{1'} + T_2 + T_{2'})|0\rangle. \quad (18)$$

$T_1$  and  $T_2$  are the standard single and double excitation operators within the HF basis, with amplitudes  $t_a^i$  and  $t_{ab}^{ij}$ , respectively,

$$T_1 = t_a^i a_i^a, \quad (19)$$

$$T_2 = t_{ab}^{ij} a_{ij}^{ab}. \quad (20)$$

The single excitations outside the HF basis,  $T_{1'}$ , are parameterized by excitations into the CABS orbitals with amplitudes  $t_{a'}^i$

$$T_{1'} = t_{a'}^i a_i^{a'}. \quad (21)$$

The double excitations outside the HF basis are parameterized by double excitations into the set of F12 basis functions  $|w_{xy}\rangle$  [eq. (1)], with amplitudes  $c_{xy}^{ij}$

$$T_{2'} = c_{xy}^{ij} w_{\alpha\beta}^{xy} a_{ij}^{\alpha\beta}, \quad (22)$$

$$w_{\alpha\beta}^{xy} = \langle \alpha\beta | w_{xy} \rangle. \quad (23)$$

An F12 double excitation can be viewed as a physically motivated linear combination of double excitations into orbitals of the complete basis. No spin restrictions are enforced on the amplitudes  $t_a^i$ ,  $t_{a'}^i$ ,  $t_{ab}^{ij}$ , or  $c_{xy}^{ij}$ . We remind the reader of the implied summation in eqs. (19)–(22) and that our convention requires  $x < y$ ,  $i < j$ , and  $\alpha < \beta$ .

### The Energy and Amplitude Equations

The second-order energy correction is given by

$$E^2 = \langle 0 | [\hat{F}^1, T_1 + T_{1'}] + [\hat{G}, T_2 + T_{2'}] | 0 \rangle \\ = f_a^i t_a^i + f_i^a t_{a'}^i + g_{ij}^{ab} t_{ab}^{ij} + V_{ij}^{\dagger xy} c_{xy}^{ij}, \quad (24)$$

The first-order amplitude equations for the singles are entirely decoupled from the doubles and are given by

$$0 = \langle 0 | a_a^i (\hat{F}^1 + [\hat{F}^0, T_1 + T_{1'}]) | 0 \rangle \\ = f_a^i + f_a^b t_b^i + f_a^b t_b^i - t_a^j f_j^i, \quad (25)$$

$$0 = \langle 0 | a_a^i (\hat{F}^1 + [\hat{F}^0, T_1 + T_{1'}]) | 0 \rangle \\ = f_a^i + f_a^b t_b^i + f_a^b t_b^i - t_a^j f_j^i. \quad (26)$$

Note that we have not assumed canonical or semicanonical orbitals. The first-order doubles amplitudes are determined by

$$0 = \langle 0 | a_{ab}^{ij} (\hat{G} + [\hat{F}^0, T_2 + T_{2'}]) | 0 \rangle \\ = g_{ab}^{ij} + f_a^c t_{cb}^{ij} + f_b^d t_{ad}^{ij} + C_{ab}^{xy} c_{xy}^{ij} - t_{ab}^{kj} f_k^i - t_{ab}^{il} f_l^j, \quad (27)$$

$$0 = w_{xy}^{\alpha\beta} \langle 0 | a_{\alpha\beta}^{ij} (\hat{G} + [\hat{F}^0, T_2 + T_{2'}]) | 0 \rangle \\ = V_{xy}^{ij} + C_{xy}^{\dagger ab} t_{ab}^{ij} + B_{xy}^{vw} c_{vw}^{ij} - X_{xy}^{vw} c_{vw}^{kj} f_k^i - X_{xy}^{vw} c_{vw}^{il} f_l^j. \quad (28)$$

Explicit expressions for  $B$ ,  $V$ ,  $X$ , and  $C$  are given later in this article. It is convenient to partition the MP2-F12 energy into the standard MP2 energy and an F12 correction. The standard MP2 energy is

$$E_{\text{MP2}} = E^0 - f_a^i \{ \varepsilon^{-1} \}_{ja}^{ib} f_b^j - g_{ij}^{ab} \{ \varepsilon^{-1} \}_{klab}^{ijcd} g_{cd}^{kl}, \quad (29)$$

and is computed very efficiently in the usual way<sup>26,27</sup> using (semi-) canonical orbitals, where

$$\varepsilon_{ib}^{ja} = (\varepsilon_a - \varepsilon_i) \delta_i^j \delta_b^a, \quad (30)$$

$$\varepsilon_{ijkl}^{klab} = (\varepsilon_a + \varepsilon_b - \varepsilon_i - \varepsilon_j) \delta_i^k \delta_j^l \delta_c^a \delta_d^b. \quad (31)$$

The MP2-F12 energy then becomes

$$E_{\text{MP2-F12}} = E_{\text{MP2}} + \tilde{f}_i^a t_{a'}^i + \tilde{V}_{ij}^{\dagger xy} c_{xy}^{ij} \\ = E_{\text{MP2}} + \Delta E_{\text{CABS}} + \Delta E_{\text{F12}}, \quad (32)$$

where

$$\tilde{f}_i^a = f_a^i - f_a^a \{ \varepsilon^{-1} \}_{ja}^{ib} f_b^j, \quad (33)$$

$$\tilde{V}_{xy}^{\dagger ij} = V_{xy}^{ij} - C_{xy}^{\dagger ab} \{ \varepsilon^{-1} \}_{klab}^{ijcd} g_{cd}^{kl}. \quad (34)$$

The final working equations to determine the amplitudes are

$$0 = R_{a'}^i = f_a^b t_b^i - t_a^j f_j^i - f_a^a \{ \varepsilon^{-1} \}_{ja}^{ib} f_b^j + \tilde{f}_i^a, \quad (35)$$

$$0 = R_{xy}^{ij} = B_{xy}^{vw} c_{vw}^{ij} - X_{xy}^{vw} c_{vw}^{kj} f_k^i - X_{xy}^{vw} c_{vw}^{il} f_l^j \\ - C_{xy}^{\dagger ab} \{ \varepsilon^{-1} \}_{klab}^{ijcd} C_{cd}^{vw} c_{vw}^{kl} + \tilde{V}_{xy}^{\dagger ij}. \quad (36)$$

With respect to the geminal contribution, eq. (36) may be solved directly (orbital-invariant ansatz), or within a minimal space of geminal functions (orbital-variant ansatz), or simply evaluated using a predetermined set of amplitudes (fixed amplitude ansatz). Furthermore, a series of approximations can be applied, where successive terms are dropped from the amplitude equations. These are detailed in the section on approximations.

### The Orbital-Invariant Optimized Ansatz

Solving eq. (36) optimizes the MP2 energy with respect to the full space of geminal functions. The energy obtained is invariant to rotations of occupied orbitals and is size extensive. However, in contrast to standard MP2 theory, the cost scales with system size as  $n^6$ , both for the construction of the intermediates  $B$ ,  $V$ ,  $X$ , and  $C$ , and also for solving eq. (36).

### The Diagonal Orbital-Variant Ansatz

The diagonal ansatz is defined by choosing

$$c_{xy}^{ij} = c_{ij}^{ij} (\delta_x^i \delta_y^j - \delta_y^i \delta_x^j) \quad (37)$$

(as  $i < j$  and  $x < y$ , the second delta term never contributes—it is included in eq. (37) for formal completeness). Orbital invariance is sacrificed to reduce the scaling of the MP2-F12 calculation with system size from  $n^6$  to  $n^5$ . This reduction in scaling arises from the fact that it is only necessary to compute the diagonal elements of the  $B$  and  $V$  matrices. However, it should be noted that  $n^6$  steps also arise when solving for the amplitudes, even for the diagonal ansatz, due to the  $C$  coupling between  $T_2$  and  $T_2'$ . To obtain  $n^5$  scaling, it is necessary to either use canonical orbitals for the calculation or to neglect the contributions from the  $C$  matrix (these are zero under the EBC). If  $C$  is neglected, the amplitude equations are

$$0 = B_{ij}^{ij} c_{ij}^{ij} - X_{ij}^{kj} c_{kj}^{ki} - X_{ij}^{il} c_{il}^{lj} + V_{ij}^{ij}. \quad (38)$$

If canonical orbitals are used, then the  $C$  coupling can be included at  $n^5$  cost by replacing  $V$  with  $\tilde{V}$  of eq. (34) and  $B$  with  $\tilde{B}$ , where

$$\tilde{B}_{ij}^{ij} = B_{ij}^{ij} - C_{ij}^{\dagger ab} \{ \varepsilon^{-1} \}_{ijab} C_{ab}^{ij}. \quad (39)$$

The first-order F12 amplitudes  $c_{xy}^{ij}$  become increasingly diagonally dominant as the orbital basis approaches completeness, or if the occupied orbitals are localized (recall that we choose  $xy = ij$ ). Local methods are currently not implemented for standard MP2 and consequently the diagonal ansatz is of limited use. We recommend the fixed-amplitude approach, which has the same computational scaling as the diagonal ansatz, while being also orbital invariant.

### The Fixed-Amplitude Ansatz

In the fixed-amplitude ansatz the amplitudes  $c_{xy}^{ij}$  for the F12 geminal basis functions are not optimized, but are simply chosen such that the first-order  $s$ - and  $p$ -wave coalescence conditions are satisfied. For the definition of the F12 amplitudes in eq. (1), this means that

$$c_{xy}^{ij} = \delta_x^i \delta_y^j. \quad (40)$$

The geminal contribution to the energy is evaluated through the Hylleraas functional, that is, the Lagrangian where the Lagrange multipliers have been replaced with the amplitudes (they are equal at first-order in perturbation theory)

$$\begin{aligned} \Delta E_{F12} &= \tilde{V}_{ij}^{\dagger xy} c_{xy}^{ij} + c_{ij}^{\dagger xy} R_{xy}^{ij} \\ &= \tilde{B}_{ij}^{ij} - X_{ij}^{kj} f_k^i - X_{ij}^{il} f_l^j + 2\tilde{V}_{ij}^{ij}. \end{aligned} \quad (41)$$

Note that although the geminal contribution is kept fixed, the amplitudes  $t_{ab}^{ij}$  are optimized and differ from those of a standard MP2 calculation through the coupling terms

$$t_{ab}^{ij} = -(\rho_{cd}^{kl} + C_{cd}^{xy} c_{xy}^{kl}) \{ \varepsilon^{-1} \}_{klab}. \quad (42)$$

### Open-Shell Considerations

The presence of the  $\hat{S}_{xy}$  operator in the definition of the F12 geminals ensures that the above three variants transfer transparently to the open-shell case. The amplitudes that satisfy the  $s$ - and  $p$ -wave coalescence conditions for the first-order wave function are still  $c_{xy}^{ij} = \delta_x^i \delta_y^j$ , and the fixed-amplitude ansatz is still a special case of the other two approaches, just as for closed-shell calculations. For unrestricted open-shell references, the  $\hat{S}_{xy}$  operator generates spin-flipped orbitals and the cost of computing the integrals is increased by a factor of two compared with an analogous calculation that does not include the spin-flipped orbitals. There are two possibilities to avoid this factor of two increase in cost. The first is to use the ROHF reference with restricted rather than semicanonical orbitals such that the spin up and down orbitals are the same. The only drawback is that Fock matrix coupling elements  $f_a^i$  are neglected in a frozen-core calculation, but these are expected to be small. Alternatively, one can choose

$$\hat{S}'_{xy} |xy\rangle = \frac{1}{2} |xy\rangle + \frac{1}{8} \sum_{vw} (s_{wx}^v s_{vy}^w - \bar{s}_{vx}^w \bar{s}_{wy}^v) |vw\rangle, \quad (43)$$

with

$$s_{wx}^v = \langle \varphi_w \sigma_v | \varphi_x \sigma_x \rangle, \quad \bar{s}_{wx}^v = s_{wz}^v s_{zx}^w. \quad (44)$$

This is the best possible choice if one does not permit spin-flipped orbitals, and the meaning can best be seen by examining the ROHF case with restricted orbitals:

$$\hat{S}'_{xy} |xy\rangle = \frac{1}{4} |xy\rangle \quad \alpha\alpha, \beta\beta \quad (45)$$

$$\hat{S}'_{xy} |xy\rangle = \left( \frac{3}{8} + \frac{1}{8} \hat{P}_{xy} \right) |xy\rangle \quad \alpha\beta \text{ "d"} \quad (46)$$

$$\hat{S}'_{xy} |xy\rangle = \frac{1}{2} |xy\rangle \quad \alpha\beta \text{ "s"} \quad (47)$$

"d" and "s" indicate doubly and singly occupied orbitals, respectively. The treatment of singly and doubly occupied orbitals is clearly unbalanced and the more rigorous approach using eq. (6) is recommended.

### CABS Singles

The energy  $\Delta E_{CABS}$  in eq. (32) is referred to as the CABS singles correction. The amplitude equations (35) have obvious similarities to the doubles equations (36) and may be solved in an analogous

way. For RHF and UHF references, this is a purely HF contribution (no correlation) and is a second-order correction to reduce the basis set error in the HF energy. For ROHF references, where  $f_a^i$  is nonzero, the CABS singles energy corrects for the basis set error in both the HF energy and the singles contribution to the ROHF-UMP2 correlation energy. It also introduces spin contamination. Although the CABS singles correction is entirely distinct from the F12 energy correction, all of the quantities required for its evaluation can be found among the MP2-F12 intermediates. If the CABS singles correction is ignored, then the basis set error in the HF contribution limits the accuracy of an F12 calculation when double- or triple-zeta orbital basis sets are used. Including the CABS singles correction essentially eliminates this source of error.

### B, V, X, and C

The  $B$ ,  $X$ ,  $C$ , and  $V$  matrices are defined as

$$B_{xy}^{vw} = \hat{S}_{xy} \hat{S}_{vw} \langle xy | f_{12} \hat{Q}_{12} \hat{F}_{12}^0 \hat{Q}_{12} f_{12} | vw \rangle, \quad (48)$$

$$X_{xy}^{vw} = \hat{S}_{xy} \hat{S}_{vw} \langle xy | f_{12} \hat{Q}_{12} f_{12} | vw \rangle, \quad (49)$$

$$C_{ab}^{xy} = \hat{S}_{xy} \langle ab | \hat{F}_{12}^0 \hat{Q}_{12} f_{12} | xy \rangle, \quad (50)$$

$$V_{xy}^{ij} = \hat{S}_{xy} \langle xy | f_{12} \hat{Q}_{12} r_{12}^{-1} | ij \rangle, \quad (51)$$

where  $\hat{F}_{12}^0 = \hat{F}_1^0 + \hat{F}_2^0$ . The three- and four-electron integrals intrinsic to these quantities are approximated as sums of products of two-electron integrals by making approximations for the strong-orthogonality projector:

$$\hat{Q}_{12} \stackrel{RI}{\approx} \hat{Q}_{12}^A = 1 - \hat{P}_1 \hat{P}_2 - \hat{O}_1 \hat{V}_2' - \hat{V}_1' \hat{O}_2, \quad (52)$$

$$\hat{Q}_{12} \stackrel{RI}{\approx} \hat{Q}_{12}^B = \hat{P}_1 \hat{V}_2' + \hat{V}_1' \hat{P}_2 + \hat{V}_1' \hat{V}_2'. \quad (53)$$

$\hat{P} = \hat{O} + \hat{V}$  and  $\hat{V}'$  projects onto the space of CABS virtuals

$$\hat{V}' = |a'\rangle\langle a'|. \quad (54)$$

$\hat{Q}_{12}^A$  is used for the  $X$  and  $V$  matrices and  $\hat{Q}_{12}^B$  is used for the  $C$  matrix. To evaluate the  $B$  matrix, we commute the Fock operator as follows

$$\begin{aligned} & \langle xy | f_{12} \hat{Q}_{12} \hat{F}_{12}^0 \hat{Q}_{12} f_{12} | vw \rangle \\ &= \frac{1}{2} \langle xy | f_{12} \hat{Q}_{12} [\hat{F}_{12}^0, \hat{Q}_{12}] f_{12} | vw \rangle + \frac{1}{2} \langle xy | f_{12} [\hat{Q}_{12}, \hat{F}_{12}^0] \hat{Q}_{12} f_{12} | vw \rangle \\ &+ \frac{1}{2} \langle xy | f_{12} \hat{Q}_{12} [\hat{F}_{12}^0, f_{12}] | vw \rangle + \frac{1}{2} \langle xy | [f_{12}, \hat{F}_{12}^0] \hat{Q}_{12} f_{12} | vw \rangle \\ &+ \frac{1}{2} \langle xy | f_{12} \hat{Q}_{12} f_{12} \hat{F}_{12}^0 | vw \rangle + \frac{1}{2} \langle xy | \hat{F}_{12}^0 f_{12} \hat{Q}_{12} f_{12} | vw \rangle. \quad (55) \end{aligned}$$

We then insert

$$\begin{aligned} \hat{Q}_{12} [\hat{F}_{12}^0, \hat{Q}_{12}] &= -(1 - \hat{P}_1) \hat{F}_1^0 \hat{V}_1' \hat{V}_2' - \hat{V}_1' (1 - \hat{P}_2) \hat{F}_2^0 \hat{V}_2' \\ &\stackrel{RI}{\approx} -\hat{V}_1' \hat{F}_1^0 \hat{V}_1' \hat{V}_2' - \hat{V}_1' \hat{V}_2' \hat{F}_2^0 \hat{V}_2', \quad (56) \end{aligned}$$

$$\begin{aligned} \hat{Q}_{12} [\hat{F}_{12}^0, f_{12}] &= \hat{Q}_{12} [\hat{T}_{12} - \hat{K}_{12} - \hat{F}_{12}^1 + \hat{U}_{12}, f_{12}] \\ &\stackrel{RI}{\approx} \hat{Q}_{12}^A [\hat{T}_{12}, f_{12}] - \hat{Q}_{12}^B (\hat{K}_{12} + \hat{F}_{12}^1 - \hat{U}_{12}) f_{12} \\ &+ \hat{Q}_{12}^A f_{12} (\hat{K}_{12} + \hat{F}_{12}^1 - \hat{U}_{12}), \quad (57) \end{aligned}$$

$$f_{12} \hat{Q}_{12} f_{12} \stackrel{RI}{\approx} f_{12} \hat{Q}_{12}^A f_{12}, \quad (58)$$

where  $\hat{T}_{12} = \hat{T}_1 + \hat{T}_2$ , and similarly for  $\hat{K}_{12}$ ,  $\hat{F}_{12}^1$ , and  $\hat{U}_{12}$ . Two-electron integrals over  $[[f_{12}, \hat{T}_1], f_{12}] = [[f_{12}, \hat{T}_2], f_{12}] = (\hat{V}_{1f_{12}}^2)^2$  and  $f_{12}^2$  can be evaluated analytically. To evaluate the remaining integrals, for example over  $\hat{P}_1 \hat{P}_2 \hat{T}_1 f_{12}$ , or  $f_{12}^2 \hat{K}_1$ , a further approximate RI over orbitals  $p'$  is inserted, which can be formulated as an orbital transformation. This leads to the following expressions for eqs. (48)–(51):

$$B_{xy}^{vw} = \frac{1}{2} \bar{B}_{xy}^{vw} + \frac{1}{2} \bar{B}_{vw}^{xy}, \quad (59)$$

$$\bar{B}_{xy}^{vw} = \bar{T}_{xy}^{vw} + X_{xy}^{vw} + X_{xy}^{vw} - \bar{P}_{xy}^{vw} + \bar{Q}_{xy}^{vw} - \bar{E}_{xy}^{vw}, \quad (60)$$

$$\bar{T}_{xy}^{vw} = \tau_{xy}^{vw} - r_{xy}^{pq} t_{pq}^{vw} - r_{xy}^{a'o} t_{a'o}^{vw} - r_{xy}^{ob'} t_{ob'}^{vw}, \quad (61)$$

$$\bar{P}_{xy}^{vw} = r_{xy}^{a'b'} p_{a'b'}^{vw} + r_{xy}^{a'b} p_{a'b}^{vw} + r_{xy}^{ab'} p_{ab'}^{vw}, \quad (62)$$

$$\bar{Q}_{xy}^{vw} = \pi_{xy}^{vw} - r_{xy}^{pq} q_{pq}^{vw} - r_{xy}^{a'o} q_{a'o}^{vw} - r_{xy}^{ob'} q_{ob'}^{vw}, \quad (63)$$

$$\bar{E}_{xy}^{vw} = C_{xy}^{ab} r_{ab}^{vw}, \quad (64)$$

$$X_{xy}^{vw} = x_{xy}^{vw} - r_{xy}^{pq} r_{pq}^{vw} - r_{xy}^{a'o} r_{a'o}^{vw} - r_{xy}^{ob'} r_{ob'}^{vw}, \quad (65)$$

$$C_{ab}^{xy} = r_{ab}^{xy} + r_{ab}^{xy}, \quad (66)$$

$$V_{xy}^{ij} = v_{xy}^{ij} - r_{xy}^{pq} g_{pq}^{ij} - r_{xy}^{a'o} g_{a'o}^{ij} - r_{xy}^{ob'} g_{ob'}^{ij}, \quad (67)$$

where we have omitted the dagger from the  $r_{xy}^{a'b'}$  for the sake of esthetical clarity and

$$\tau_{xy}^{vw} = \frac{1}{2} \hat{S}_{xy} \hat{S}_{vw} \langle xy | [[f_{12}, \hat{T}_{12}], f_{12}] | vw \rangle, \quad (68)$$

$$\pi_{xy}^{vw} = \hat{S}_{xy} \hat{S}_{vw} (\langle xy | f_{12}^2 | \bar{v}w \rangle + \langle xy | f_{12}^2 | \bar{w}v \rangle), \quad (69)$$

$$x_{xy}^{vw} = \hat{S}_{xy} \hat{S}_{vw} \langle xy | f_{12}^2 | vw \rangle, \quad (70)$$

$$v_{xy}^{ij} = \hat{S}_{xy} \langle xy | f_{12} r_{12}^{-1} | ij \rangle, \quad (71)$$

$$r_{p'q'}^{vw} = \hat{S}_{vw} \langle p'q' | f_{12} | vw \rangle, \quad (72)$$

$$t_{p'q'}^{vw} = r_{p'q'}^{vw} + r_{p'q'}^{vw} - r_{p'q'}^{vw} - r_{p'q'}^{vw}, \quad (73)$$

$$p_{p'q'}^{vw} = r_{p'q'}^{vw} + r_{p'q'}^{vw}, \quad (74)$$

$$q_{p'q'}^{vw} = r_{p'q'}^{vw} + r_{p'q'}^{vw}. \quad (75)$$

The transformed orbitals are defined as

$$|\check{x}\rangle = f_{p'}^{0x} |p'\rangle, \quad (76)$$

$$|\bar{x}\rangle = t_{p'}^x |p'\rangle, \quad (77)$$

$$|\tilde{x}\rangle = (k_{p'}^x + f_{p'}^{1x} - u_{p'}^x) |p'\rangle, \quad (78)$$

$$|\check{a}\rangle = f_a^{0a'} |a'\rangle. \quad (79)$$

**Table 2.** Scaling and CABS Convergence Properties of MP2-F12 Variants.

Method	Orb. <sup>a</sup>	Scaling with system size			RI truncation for the atomic case	
		Fixed	Noinv	Inv	$L_{\max}$	Term responsible
2A*	c	$n^5$	$n^5$	$n^6$	$\max [2L_{\text{occ}} + L_{\text{vir}}^b, 3L_{\text{occ}}]$	$t_{pq}^{vw}, t_{xy}^{a'o}$
	nc	$n^5$	$n^5$	$n^6$		
2A	c	$n^5$	$n^5$	$n^6$	$2L_{\text{occ}} + L_{\text{vir}}$	$C_{ab}^{xy}$
	nc	$n^5$	$n^6$	$n^6$		
2B	c	$n^5$	$n^5$	$n^6$	$\infty^{c,d}$	$P_{a'b'}^{vw}$
	nc	$n^5$	$n^6$	$n^6$		

<sup>a</sup>c refers to (semi-) canonical orbitals (r12orb=hf), nc to all other choices.

<sup>b</sup>If  $t = h$  rather than  $t = f + k$ , this reduces to  $\min[L_{\text{vir}} + 2, 2L_{\text{occ}} + L_{\text{vir}}]$ .

<sup>c</sup>Rapidly convergent  $(L + 1)^{-7}$ . See Ref. 28.

<sup>d</sup>If  $p_{a'b'}^{vw}$  is neglected (not implemented), this becomes  $2L_{\text{occ}} + L_{\text{vir}}$ .

$L_{\max}$  is the maximum angular momentum quantum number that contributes to the CABS RI insertion for an atom.  $L_{\text{occ}}$  and  $L_{\text{vir}}$  are the maximum angular momentum quantum numbers of the occupied and virtual orbitals, respectively.

The orbital transformation matrix  $t$ , used for the commutator  $[\hat{T}_{12}, f_{12}]$ , is best chosen as  $t = h + j$ . This is referred to as the F + K commutator approximation (note that  $h + j = f + k - u$ ). For calculations where the exchange terms are neglected, there is a slight computational advantage when choosing  $t = h$  instead (T + V). We now elucidate the steps required to arrive at eqs. (59)–(79) through an example. Consider the following contribution to  $\hat{T}_{xy}^{vw}$

$$\begin{aligned} & \hat{S}_{xy} \hat{S}_{vw} \langle xy | f_{12} \hat{P}_1 \hat{P}_2 [\hat{T}_{12}, f_{12}] | vw \rangle \\ &= \hat{S}_{xy} \hat{S}_{vw} \sum_{pq} \langle xy | f_{12} | \phi_p \phi_q \rangle \langle \phi_p \phi_q | [\hat{T}_{12}, f_{12}] | vw \rangle \\ &= \hat{S}_{xy} \hat{S}_{vw} \sum_{pq} \frac{1}{2} \langle xy | f_{12} | pq \rangle \langle pq | [\hat{T}_{12}, f_{12}] | vw \rangle \\ &= \hat{S}_{xy} \hat{S}_{vw} \sum_{p < q} \langle xy | f_{12} | pq \rangle \langle pq | [\hat{T}_{12}, f_{12}] | vw \rangle, \end{aligned} \quad (80)$$

$$\stackrel{RI}{\approx} r_{xy}^{pq} t_{pq}^{vw}. \quad (81)$$

We remind the reader of our pair index convention, where contractions such as  $r_{xy}^{pq} t_{pq}^{vw}$  imply a summation range  $p < q$ , where the indices  $p$  and  $q$  each run over both the  $\alpha$  and  $\beta$  spin orbitals.

Several aspects of the above choices in approximation require explanation. First, the Fock operator is commuted [eq. (55)] rather than inserting two approximate RI expansions because the double RI for the  $f_{12} \hat{T}_{12} f_{12}$  converges as  $l^{-1}$ , where  $l$  is the highest angular momentum operator in the  $p'$  basis. This slow CABS convergence is avoided because the corresponding commutator integral can be evaluated analytically. Second, we evaluate the commutator  $\hat{Q}_{12}[\hat{K}_{12}, f_{12}]$  as  $\hat{Q}_{12}^B \hat{K}_{12} f_{12} - \hat{Q}_{12}^A f_{12} \hat{K}_{12}$  rather than as  $\hat{Q}_{12}^B[\hat{K}_{12}, f_{12}]$ . While the latter choice is more consistent and leads to shorter expressions and a saving of 15% in CPU time, it involves a double RI for the integrals  $f_{12} f_{12} \hat{K}_{12}$ , which is also slowly convergent with CABS and leads to sizable CABS errors.<sup>28</sup> All of the RI insertions in the computational scheme detailed above have partial wave expansions that either truncate or are rapidly convergent. A summary of the CABS convergence behavior for various MP2-F12 approaches is given in Table 2. Finally, as an aside, we note that

$\langle xy | f_{12} \hat{Q}_{12} \hat{F}_{12}^1 \hat{Q}_{12} f_{12} | vw \rangle = 0$ . The presence of the GBC terms in the  $B$  matrix is a consequence of the commutator approach, and they arise independently of the choice of zeroth-order partitioning of the Fock matrix.

### Spin-Adaption

Equations (61)–(67) are in spin orbital formulation and give compact expressions suitable for implementation of UHF-MP2-F12. Spin integration restricts the pairs  $xy$  and  $vw$  to have the same spin component as the pair  $ij$  and, similarly, the contraction ranges within  $p'q'$  are restricted to pairs with the same spin components as  $ij$ . Separate amplitude equations are thus solved for the three spin cases, leading to three uncoupled energy contributions. It should also be noted that for pairs  $ij$  with like spins, applying the summation convention and spin integration eliminates the last contraction in each of eqs. (61)–(63), (65), and (67). Furthermore, as for the like-spin pairs,

$$\hat{S}_{vw} \langle p'q' | f_{12} | vw \rangle = \frac{1}{4} \langle p'q' | f_{12} | vw \rangle, \quad (82)$$

it is more convenient to collect all the factors of  $\frac{1}{4}$  and apply them once at the end, by absorbing them into the amplitudes. Thus, for fixed amplitudes of like-spin pairs, we modify our definitions to  $\hat{S}_{vw} = \frac{3}{2} + \frac{1}{2} \hat{P}_{vw}$  and  $c_{xy}^{ij} = \frac{1}{4} \delta_x^i \delta_y^j$ .

For ROHF-MP2-F12 a significant computational saving ( $\sim 50\%$ ) is gained by using restricted orbitals rather than semicanonicalized orbitals. This arises primarily from the simplification in the terms generated by  $\hat{S}_{vw}$  on the spin-opposite pairs (see section on open-shell considerations). An optimal implementation would involve recasting the contributions into parts that are the same for the  $\alpha\alpha$ ,  $\beta\beta$ , and  $\alpha\beta$  pairs, and parts that are different. This is not done in TURBOMOLE and ROHF-MP2-F12 is implemented using eqs. (59)–(79). The default is to use semicanonical orbitals.

For RHF-MP2-F12, the  $\alpha$  and  $\beta$  orbitals are identical and the energy decomposes into singlet and triplet pair energies. The  $\alpha\alpha$ ,  $\beta\beta$ , and  $\alpha\beta + \beta\alpha$  triplet components are degenerate, and the energy and amplitude expressions are exactly those of the like-spin UHF-MP2-F12 case. The singlet energy and amplitude expressions are

uncoupled from the triplet pairs and have identical structure to the triplet equations, with two important differences. First, all of the antisymmetric two-electron quantities in the triplet expressions are replaced by symmetric quantities, for example,

$$r_{p'q'}^{vw} = \hat{S}_{vw} (\langle \phi_{p'} \phi_{q'} | f_{12} | \phi_v \phi_w \rangle + \langle \phi_{p'} \phi_{q'} | f_{12} | \phi_w \phi_v \rangle) \times (1 + \delta_{p'q'})^{-1/2} (1 + \delta_{vw})^{-1/2}. \quad (83)$$

Second, the pair indices run over  $i \leq j$ , where  $i$  and  $j$  are orbital indices rather than spin orbital indices. Similarly, the pair contractions run over  $p' \leq q'$ , with orbital indices  $p'$  and  $q'$ . A straightforward way to derive the singlet energy and amplitude equations is to begin with the spin orbital case and to notice that the  $\alpha\beta$  pairs decompose into triplet and singlet spin-adapted pairs through the transformation

$$\frac{1}{\sqrt{2}}(|ij\rangle - |ji\rangle) = \frac{1}{2}(\varphi_i\varphi_j - \varphi_j\varphi_i)(\alpha\beta + \beta\alpha), \quad (84)$$

$$(2 + 2\delta_{ij})^{-1/2}(|ij\rangle + |ji\rangle) = (2 + 2\delta_{ij})^{-1/2}(\varphi_i\varphi_j + \varphi_j\varphi_i)(\alpha\beta - \beta\alpha). \quad (85)$$

The singlet and triplet energies and amplitude equations are recovered by applying this transformation to the spin orbital energy and amplitude equations for the  $\alpha\beta$  pairs. For singlet spin-adapted pairs, the effect of  $\hat{S}_{vw}$  in eq. (83) is only to introduce a factor of  $\frac{1}{2}$ . It is more convenient to collect all the factors of  $\frac{1}{2}$  and apply them once at the end, by absorbing them into the amplitudes. Thus, for fixed amplitudes of singlet pairs, we use  $\hat{S}_{vw} = \frac{3}{4} + \frac{1}{4}\hat{P}_{vw}$  and  $c_{xy}^{ij} = \frac{1}{2}(\delta_x^i\delta_y^j + \delta_x^j\delta_y^i)(1 + \delta_{ij})^{-1/2}(1 + \delta_{xy})^{-1/2}$  (note that because  $i \leq j$  and  $x \leq y$  this reduces to  $c_{xy}^{ij} = \frac{1}{2}\delta_x^i\delta_y^j$ ).

### Density Fitting

Density fitting (DF) is a standard device in computational chemistry, used to greatly reduce the prefactor for integral evaluation and transformation steps. The overlap distribution of orbitals  $ip$  and  $jq$  are fitted using a dedicated auxiliary fitting basis  $\{Q\}$  such that the integrals  $(ip|g_{12}|jq)$  are approximated as<sup>29</sup>

$$(ip|g_{12}|jq) \approx \sum_{PQR} [(ip|g_{12}|Q)(Q|P)^{-1/2}] [(P|R)^{-1/2}(R|g_{12}|jq)] = G_{ip,P}G_{jq,P}, \quad (86)$$

where  $(P|Q)$  is shorthand for the Coulomb metric  $(P|g_{12}|Q)$ , with  $g_{12} = r_{12}^{-1}$ . Evaluation of electron repulsion integrals between Gaussian charge distributions for the three-index  $G_{\mu\nu,P}$  intermediates is much cheaper than for the  $(\mu\nu|g_{12}|\kappa\lambda)$  AO integrals. Furthermore, the transformation from atomic to molecular orbitals is performed on three-index rather than four-index quantities. The only  $n^5$  scaling step is then the final contraction to form the target integrals, which has a low prefactor and is well suited to the use of optimized linear-algebra routines. Disk requirements can also be greatly reduced by avoiding the storage of four-index matrices, but rather computing them on the fly when needed from three-index intermediates stored

on disk. DF is also known as the RI approximation in the literature, but in the context of F12 theory, where there are RI approximations for the three- and four-electron integrals, we use the term density fitting to avoid confusion.

Equation (86) ensures that the error in the energy is quadratic in the density-fitting error and is therefore referred to as robust. The generalization of robust density fitting to the two-electron integrals required in MP2-F12 theory was developed by Manby<sup>30</sup> and can be cast into such a form that the number of transformation and contraction steps is minimal,<sup>31</sup>

$$(ip|f_{12}|jq) \approx G_{ip,P}R_{jq,P} + R_{ip,P}G_{jq,P} - G_{ip,P}U_{P,Q}G_{jq,Q} = G_{ip,P}\tilde{R}_{jq,P} + \tilde{R}_{ip,P}G_{jq,P}, \quad (87)$$

where

$$U_{P,Q} = (P|R)^{-1/2}(R|f_{12}|S)(S|Q)^{-1/2}, \quad (88)$$

$$\tilde{R}_{ip,Q} = R_{ip,Q} - \frac{1}{2}G_{ip,P}U_{P,Q}, \quad (89)$$

$$R_{ip,Q} = (ip|f_{12}|R)(R|Q)^{-1/2}, \quad (90)$$

$$G_{ip,Q} = (ip|g_{12}|R)(R|Q)^{-1/2}. \quad (91)$$

The above equations also hold if  $f_{12}$  is everywhere replaced by any of the  $(\hat{\nabla}_1 f_{12})^2, f_{12}^2$ , or  $f_{12}g_{12}$  operators required for the  $\tau, \pi, x$ , and  $\nu$  matrices. Moreover, the formulation also applies to any of the transformed orbitals, compare eqs. (76)–(79). The computational effort of computing the intermediates  $\tilde{R}_{ip,Q}$  is negligible, and the F12 integrals are only twice as expensive as the electron repulsion integrals.

### Approximations

Distinct from the RI approximation, intrinsic to the F12 approach, and the DF approximation, used to reduce the cost of the integral evaluation and transformation, a great number of approximations have arisen in F12 theory, where certain terms are neglected from the energy and amplitude equations. The purpose of these was to simplify the equations and further reduce the computational cost, while preserving accuracy. The method in which the MP2-F12 energy is computed as outlined above without further simplification is referred to as approximation B, or equivalently approximation C (see section on the connection with other approximations). The multitude of alternative approximations has now been whittled down to two useful simplifications.

#### Approximation A

In approximation A, we make the replacement in the residual eq. (36)

$$B_{xy}^{vw}c_{vw}^{ij} - X_{xy}^{vw}c_{vwk}^{kj}f_l^i - X_{xy}^{vw}c_{vwl}^{il}f_j^i \approx (T_{xy}^{vw} - E_{xy}^{vw})c_{vw}^{ij} \quad (92)$$

The fact that the  $[\hat{K}_{12}, f_{12}]$  term  $(P - Q)$  is small enough to be neglected can be deduced by noting that it is zero for a local exchange



operator, such as the LDA exchange functional used in density functional theory. The  $\hat{F}^1$  contributions to  $P$  and  $Q$  are zero if the GBC is fulfilled and are therefore also small. The other neglected terms involve the geminal overlap

$$\frac{1}{2}(X_{xy}^{\check{v}w} + X_{xy}^{\check{w}v} + X_{xy}^{vw} + X_{xy}^{vw})c_{vw}^{ij} - X_{xy}^{vw}c_{vw}^{kj}f_k^i - X_{xy}^{vw}c_{vw}^{il}f_l^j. \quad (93)$$

For closed shell systems in a canonical basis, this simplifies to (assuming  $xy = ij$ )

$$\frac{1}{2}(\varepsilon_x + \varepsilon_y + \varepsilon_v + \varepsilon_w - 2\varepsilon_i - 2\varepsilon_j)X_{xy}^{vw}c_{vw}^{ij}. \quad (94)$$

The diagonal elements cancel and indeed need not be computed for the diagonal or fixed amplitude ansatz. Thus, it can be seen that the overlap contribution is also usually small in the general case.

The combined neglect of the exchange and overlap contributions causes slight overshooting in the computed correlation energies. Consequently, the A and B approximations converge to the basis set limit from opposite directions and the difference between the A and B values is a useful indication of the remaining basis set error. Additionally, 0.6 A + 0.4 B gives an improved estimate of the basis set limit, at least for total energies.<sup>32</sup>

Concerning the computational cost, the most expensive contribution to approximation B comes from the  $P$  term, which requires  $O^2N^2X$  contractions to build the  $p$  matrices and further  $O^4N^2$  contractions to build the full  $P$  matrix, if the amplitudes are to be optimized in an orbital-invariant manner. Approximation A is much cheaper than B, primarily because  $P$  is neglected. However, approximation A\* is even cheaper and is in general more accurate than approximation A.

#### Approximation A\*

Approximation A\* is derived from approximation A by assuming the EBC. Note that the GBC terms have already been discarded since these correspond to the  $\hat{F}^1$  contributions to  $P$  and  $Q$ . Matrix  $C$  vanishes under the EBC and thus the residual equation (36) becomes simply

$$0 = R_{xy}^{ij} = T_{xy}^{vw}c_{vw}^{ij} + V_{xy}^{ij}, \quad (95)$$

and the energy is

$$\Delta E_{F12} = V_{ij}^{\dagger xy}c_{xy}^{ij}. \quad (96)$$

Approximation A\* is the simplest and cheapest approach and is surprisingly accurate, particularly for small orbital basis sets. The GBC and EBC assumptions can also be separately applied to approximation B to give B\*, but because the latter one is neither cheaper nor more accurate than A\*, this is not a useful approach.

The EBC assumption can also be applied to the CABS singles amplitude and energy equations, removing the contribution from  $f_a^b$  to give

$$\Delta E_{\text{CABS}} = -f_i^{a'}\{\varepsilon^{-1}\}_{a'b'}^{ib'}f_b^j \quad (97)$$

This does not lead to any computational savings and only serves to lower the accuracy. Applying the EBC in this way is somewhat incongruous with keeping the smaller GBC terms, but eq. (97) can also be derived by redefining the zeroth-order Fock operator such that the EBC terms are considered first-order in the perturbation.

There is, however, a subtle distinction between assuming the EBC and adopting the revised partitioning of the Hamiltonian operator. For approximation A, the two alternatives lead to the same equations for  $\Delta E_{F12}$ , but not for approximation B: Although all contributions involving the  $C$  matrix are then identically zero, additional terms appear due to the  $[\hat{F}^1, f_{12}]$  contribution to  $P - Q$ . This, together with the consideration of the CABS singles correction, convinces us that the zeroth-order Fock operator should contain the EBC terms, and we define approximation A\* as assuming the EBC only for the  $\Delta E_{F12}$  contribution.

#### Connection with Other Approximations

The MP2-F12 equations detailed here are very closely related, but not identical to the equations presented by Klopper and Samson in 2002.<sup>33</sup> Even adjusting for the modified definition of  $\hat{Q}_{12}$  and the CABS approach, the methods differ in three ways: (i) Here, the single-commutator  $[\hat{T}_{12}, f_{12}]$  terms are evaluated using double RI, whereas these were previously computed analytically as two-electron integrals. (ii) Here, the  $C$  matrix is evaluated by direct RI without commuting the Fock operator. Thus, the  $C$  matrix is kept the same for the A and B approximations. (iii) Here, we do not assume the GBC but compute these terms.

These differences are slight and, GBC aside, refer to the way terms are computed rather than which terms are computed, and we therefore refer to the present approach as approximation B to maintain consistency with our earlier work. However, provided that the matrix  $t = h + j$  (F + K) is used for the kinetic energy commutator [eq. (77)], the present implementation of approximation B is in fact identical to approximation C, introduced by Noga.<sup>34</sup> This becomes clear once it is realized that

$$\begin{aligned} \bar{E}_{xy}^{vw} &= \bar{T}_{xy}^{vw} + X_{xy}^{\check{v}w} + X_{xy}^{\check{w}v} - \bar{P}_{xy}^{vw} + \bar{Q}_{xy}^{vw} - \bar{E}_{xy}^{vw} \\ &= \bar{T}_{xy}^{vw} + X_{xy}^{\check{v}w} + X_{xy}^{\check{w}v} - \bar{P}_{xy}^{vw} - \bar{E}_{xy}^{vw} \\ &= \tau_{xy}^{vw} - r_{xy}^{pq}(r_{pq}^{vw} + r_{pq}^{\check{v}w}) - r_{xy}^{a'o}(r_{a'o}^{vw} + r_{a'o}^{\check{v}w}) - r_{xy}^{ob'}(r_{ob'}^{vw} + r_{ob'}^{\check{v}w}) \\ &\quad + x_{xy}^{\check{v}w} + x_{xy}^{\check{w}v} - \bar{P}_{xy}^{vw} - \bar{E}_{xy}^{vw}. \end{aligned} \quad (98)$$

The last equation is exactly equivalent to those reported by Werner et al. for approximation C.<sup>35</sup> Computing approximation B with  $t = h + j$  (i.e., approximation C) directly in this way leads to a noticeable computational saving since significantly fewer three-index intermediates are required and thus fewer contractions are performed. However, if one desires to compute energies for both approximations A and B to obtain an estimate of the remaining basis set incompleteness error, this saving is lost. Note that the equivalence of our formulas with those of Werner et al. applies only for  $\hat{U} = 0$  in eq. (10). In our work,  $\hat{U}$  is part of the Fock operator, and if  $\hat{U} \neq 0$ , then  $\hat{F} + \hat{K} \neq \hat{T} + \hat{V} + \hat{J}$ .

```
Orbital basis      : cc-pVTZ-F12
Cardinal number   : T
Recommended exponent: 1.0000
Actual exponent   : 1.0000
```

## INPUT MENU FOR MP2-F12 CALCULATIONS

```
ansatz      : CHOOSE ANSATZ          2      [1,2*,2]
r12model    : CHOOSE MODEL           B      [A,B]
comaprox    : COMMUTATOR APPROXIMATION F+K    [F+K,T+V]
cabs        : CABS ORTHOGONALIZATION svd 1.0D-08 [cho,svd]
examp       : CHOOSE FORMULATION     fixed flip [inv,fixed,noinv, flip,noflip]
r12orb      : CHOOSE GEMINAL ORBITALS hf      [hf,roh,boys,pipek]
corrfac     : CHOOSE CORRELATION FACTOR LCG    [R12,LCG]
cabsingles  : CABS SINGLE EXCITATIONS on     [on,off]
pairenergy  : PRINT OUT PAIRENERGIES off    [on,off]
slater      : SLATER EXPONENT        1.0000

* / end     : write $r12 to file and leave the menu
&          : go back - leaving $r12 unchanged...
```

**Scheme 1.** The f12 menu of the define module of TURBOMOLE.**Options and Keywords**

A MP2-F12 calculation is defined through a number of choices concerning the nature of the geminals ( $f_{12}$  and  $\hat{Q}_{12}$ ), the geminal excitation space ( $ijvw$  or  $ijj$ ), and approximations in computing the  $B$  matrix (GBC, EBC,  $[\hat{T}, f_{12}]$ ). These choices correspond to keywords in TURBOMOLE's  $\$r12$  data group, which are explained in the following.

To run a MP2-F12 calculation, one has to select three different auxiliary basis sets, namely *cbas*, *cabs*, and optionally *jkbas*. The RIC2 program uses robust fitting techniques for the F12 integrals and the *cbas* basis is used for both the F12 and the usual MP2 electron-repulsion integrals. For the density fitting of the Coulomb and exchange matrices of the Fock matrix, the *jkbas* will be used if it is included in the control file (this is recommended and is achieved using the *jkbas* submenu in the *cc* menu of *define*; the *cbas* basis will be used instead if the *jkbas* is not included). For the RI approximation of the three- and four-electron integrals as sums of products of two-electron integrals, intrinsic to the F12 method, the CABS approach is used. When *define* is used to set up the *cabs* basis, the library *cabasen* is searched. This library contains the optimized *cabs* basis sets<sup>5,6</sup> for the cc-pVXZ-F12 basis sets of Peterson et al.<sup>4,7</sup> For other basis sets, the auxiliary basis in the library *cabasen* is identical with the auxiliary basis in the library *cbas*.

The  $\$r12$  data group may be set by choosing the *f12* option in the *cc* menu when running *define*. This command activates the *f12* menu, where the default options may be changed if desired (cf. Scheme 1, a cc-pVTZ-F12 basis set was used in the example).

The keyword *ansatz* refers to the choice of  $\hat{Q}_{12}$ . Almost all modern MP2-F12 calculations use *ansatz 2* (default), which is defined in terms of  $\hat{Q}_{12}$  as given in eq. (3). Ansatz 2 gives much improved<sup>33</sup> energies over *ansatz 1*, which uses

$$\hat{Q}_{12} = (1 - \hat{P}_1)(1 - \hat{P}_2), \quad \hat{P} = \sum_p |p\rangle\langle p|. \quad (99)$$

The main additional cost of using *ansatz 2* over *ansatz 1* is concerned with the coupling between the F12 and conventional amplitudes. This coupling is avoided by choosing *2\**, which corresponds to neglecting EBC terms in the Fock matrix elements.

The keyword *r12model* refers to the method of computing the  $B$  matrices (see the section on approximations for details). The cost and accuracy increase from A to B. It is recommended to use B (default). The energies computed using A are then also printed out in the output.

The keyword *comaprox* is the method for approximately computing the integrals for the operator  $[\hat{T}, f_{12}]$ , where the matrix representations of F+K or T+V are used. F+K (the core Hamiltonian plus Coulomb term) is recommended and is the default.

The keyword *cabs* refers to the method of orthogonalizing the orbitals in the complementary auxiliary basis. Singular-value decomposition (*svd*) or Cholesky decomposition (*cho*) are available. *svd* is recommended and is the default, with a threshold of 1.0d-08. The basis set used for CABS is set from the *cc* menu.

The keyword *examp* refers to the choice of excitation space. *inv* is the orbital-invariant method, with amplitudes  $c_{vw}^{ij}$ . *noinv* is the original orbital-dependent diagonal *ijj* method of Ref. 36, with amplitudes  $c_{ij}^{ij}$  (not recommended, unless in combination with localized orbitals). *fixed* is the (diagonal and orbital-invariant) rational generator approach of Ref. 37, where the F12 amplitudes are not optimized but predetermined using the coalescence conditions (default, cf. section on the fixed-amplitude *ansatz*).

The keyword *r12orb* controls which orbitals are used in the calculation. *hf* means that (semi-) canonical Hartree-Fock orbitals are used (default). *roh* means that ROHF orbitals are used. Both the Boys<sup>38</sup> and Pipek-Mezey<sup>39</sup> methods are available for the localization of the orbitals, but this works only for closed-shell systems. It should be noted that for the orbital invariant methods, using localized and canonical orbitals give identical energies and that the noninvariant optimized method only has  $n^5$  scaling for *ansatz 2\**

**Table 3.** Frozen-Core MP2-F12/2B Second-Order Correlation Energies (in  $E_h$ ) of the O Atom in the cc-pVQZ-F12 Basis as a Function of the Keywords `r12orb` and `examp`.

<code>r12orb</code>	<code>examp</code>	MP2	F12/2B <sup>a</sup>	$E_{\text{CABS}}^b$	Total
ROHF reference, equivalent orbitals ( $E_{\text{ROHF}} = -74.8092632 E_h$ )					
rohff	inv flip	-0.1701183	-0.0089115	-0.0000173	-74.9883103
rohff	fixed flip	-0.1701183	-0.0088920	-0.0000173	-74.9882908
rohff	inv noflip	-0.1701183	-0.0087685	-0.0000173	-74.9881673
rohff	fixed noflip	-0.1701183	-0.0087000	-0.0000173	-74.9880988
hff	inv flip	-0.1701544	-0.0089127	-0.0000173	-74.9883475
hff	fixed flip	-0.1701544	-0.0088931	-0.0000173	-74.9883280
hff	inv noflip	-0.1701544	-0.0087698	-0.0000173	-74.9882046
hff	fixed noflip	-0.1701544	-0.0087014	-0.0000173	-74.9881362
ROHF reference, nonequivalent orbitals ( $E_{\text{ROHF}} = -74.8122513 E_h$ )					
rohff	inv flip	-0.1682893	-0.0088262	-0.0000188	-74.9893856
rohff	fixed flip	-0.1682893	-0.0088080	-0.0000188	-74.9893674
rohff	inv noflip	-0.1682893	-0.0086813	-0.0000188	-74.9892407
rohff	fixed noflip	-0.1682893	-0.0086136	-0.0000188	-74.9891731
hff	inv flip	-0.1683264	-0.0088274	-0.0000188	-74.9894238
hff	fixed flip	-0.1683264	-0.0088092	-0.0000188	-74.9894056
hff	inv noflip	-0.1683264	-0.0086826	-0.0000188	-74.9892791
hff	fixed noflip	-0.1683264	-0.0086150	-0.0000188	-74.9892114
UHF reference ( $E_{\text{UHF}} = -74.8188201 E_h$ )					
hff	inv flip	-0.1614851	-0.0086913	-0.0000209	-74.9890174
hff	fixed flip	-0.1614851	-0.0086737	-0.0000209	-74.9889998
hff	inv noflip	-0.1614851	-0.0085468	-0.0000209	-74.9888729
hff	fixed noflip	-0.1614851	-0.0084807	-0.0000209	-74.9888067

<sup>a</sup>Using ansatz 2, approximation B, and the F+K commutator approximation.<sup>b</sup>CABS singles contribution.

(`ansatz = 2*`) and approximation A (`r12model = A`). Pair energies (*vide infra*) can only be printed out in computations with (semi-) canonical orbitals (`r12orb = hf`). As a reference for future work, Table 3 displays the valence-shell second-order correlation energies of the neutral oxygen atom obtained using various choices for the keywords `examp` and `r12orb` in the cc-pVQZ-F12 basis. The calculations were performed in the cc-pVQZ-F12 basis of Peterson and co-workers,<sup>4</sup> using their corresponding OptRI auxiliary basis as CABS,<sup>5</sup> the aug-cc-pwCV5Z `cbas` of Ref. 40 for the (robust) fitting of both the F12 integrals and the usual electron-repulsion integrals, and the aug-cc-pV5Z `jkbas` basis of Weigend<sup>41</sup> for the Coulomb and exchange matrices of the Fock matrix.

The keyword `corrfac` corresponds to the choice of correlation factor  $f_{12}$  in the geminal basis functions. `R12` results in a calculation using linear- $r_{12}$  and `LCG` results in a calculation using the Slater-type correlation factor with appropriate exponent for the chosen basis set. This Slater-type correlation factor is represented as a linear combination of six Gaussians (see Ref. 23). Note that the exponents 0.9, 1.0, and 1.1  $a_0^{-1}$  are recommended for use with the cc-pVXZ-F12 basis sets with `X = D, T, and Q`, respectively.<sup>4</sup> The recommended values for the aug-cc-pVXZ basis sets with `X = D, T, Q, and 5` are 1.0, 1.1, 1.4, and 1.4  $a_0^{-1}$ .

The keyword `cabsingles` switches on/off the calculation of a second-order correction to the Hartree-Fock energy by accounting for single excitations into the complementary auxiliary basis set (CABS). The single excitations into the CABS basis can be

computed without extra costs if the CABS Fock matrix elements are required anyway for the F12 calculation (i.e., for `ansatz 2`, approximation B or `comapprox = F+K`). The computation of CABS singles cannot be switched off if it is free of costs.

The keyword `pairenergy` switches on/off the printing of the F12 contributions to the MP2 pair energies (default `pairenergy = off`).

By default, a data group `$lcg`, in which the represented by six Gaussians, is inserted into the control file (cf. Scheme 2, data group may be edited by the user, if required).

On the left panel of Scheme II, a linear combination of six Gaussians is used to represent a Slater-type geminal with exponent 1.0  $a_0^{-1}$ . On the right panel, the Gaussian exponents and contraction coefficients are defined for a linear combination of three Gaussians by the user.

MP2-F12 calculations may be combined with Grimme's SCS approach by inserting `scs` into the data group `$ricc2`, as indicated in Scheme 3.

```

$lcg                               $lcg
nlcg                               nlcg           3
slater  1.0000                    expo1      coef1
                                           expo2      coef2
                                           expo3      coef3

```

**Scheme 2.** Input for the correlation factor.

```
$ricc2
  mp2 energy only
  scs
```

**Scheme 3.** Input for the SCS approach.

In this case, the SCS parameters  $\text{cos} = 6/5$  and  $\text{css} = 1/3$  are used. Also individual scaling factors for the same-spin and opposite-spin contributions may be defined.

## Implementation

### Integrals

In addition to the standard electron-repulsion integrals (ERIs) between three charge distributions, required for the DF-MP2 method,

$$(\mu\nu|g_{12}|P), \quad (100)$$

the implementation of MP2-F12 requires several new kinds of integrals, where the electron repulsion operator  $g_{12}$  is replaced by each one of

$$f_{12}, \quad f_{12}^2, \quad f_{12} \cdot g_{12}, \quad (\hat{\nabla}_1 f_{12})^2. \quad (101)$$

$f_{12}$  is the correlation factor of the geminal basis functions, which is either linear in the interelectronic distance, or an arbitrary combination of Gaussians in the interelectronic distance. Within the Obara-Saika recursion method for integral evaluation, one only needs to modify the integral kernel to generate the new integral types. Thus, the MP2-F12 integrals take full advantage of the efficient Obara-Saika integral code within TURBOMOLE.

For correlation factors that are linear combination of Gaussians, the contraction of the Gaussians is performed at the level of the Boys function, which ensures that the cost for the new integrals does not scale with the number of Gaussians used in the fit and that the new integrals cost the same as conventional ERIs to within a small prefactor. Furthermore, since the Schwartz inequality applies to the resulting kernel, screening for the new integrals with a LCG correlation factor is obtained from a straightforward generalisation of the ERI case.

### Three-Index Intermediates

The construction of the basic three-index intermediates is carried out using RICC2 routines, which have been extended to be able to treat the new auxiliary basis set. Except for the novel features, all basic steps are the same as for the efficient DF-MP2 implementation. In particular, the AO-MO transformation is performed for the (transformed) occupied index first, which drastically reduces the number of matrix elements involved in the subsequent AO-MO transformation for the second index (typically virtual or CABS). When creating three-index intermediates, each block of orbital spaces required is stored separately in order to increase disk I/O efficiency when building four-index quantities.

### Semidirect Algorithm

Some of the core aims of the TURBOMOLE program package are the low resource requirements, ability to run calculations on large molecules on desktop machines and a parallel implementation with a high speed-up. For the MP2 algorithm this translates into using an algorithm that needs to store only three-index quantities on hard disk. Therefore, four-index integrals are computed by DF and are directly used in the construction of the  $B$ - and  $V$ -type matrices without storing them on disk. The reduced disk requirements make the calculation of large molecules possible and the reduced disk I/O ensures a high speed-up in parallel calculations. Although calculation of MP2-F12 energies for ansatz 2 and approximation B with all amplitudes optimized scales as  $n^6$  with system size, several MP2-F12 variants permit a lower  $n^5$  scaling algorithm and the lower scaling algorithm, is implemented wherever possible (see Table 2).

In the following, we outline the algorithm to compute matrices such as  $V$  and  $B$ . After the computation of the three-index integrals needed for the construction of the four-index quantities via DF (see section on density fitting), the integrals are resorted such that the virtual index is the outermost index (the auxiliary index is always fastest). For closed-shell calculations, the three-index integrals are read from disk and are contracted ( $n^5$ ) to the four-index integrals, such as  $(xp|yq)$  or  $(ip|jq)$ . The (spatial) orbital indices run over the triangle  $p \leq q$  and the square  $x, y$  or  $i, j$ . Then the indices  $x, y$  or  $i, j$  are (anti-) symmetrized to yield the intermediates

$$\tilde{a}_{ij}^{pq} = (a_{ij}^{pq} \pm a_{ji}^{pq})(1 + \delta_{ij})^{-1/2}(1 + \delta_{pq})^{-1/2}, \quad (102)$$

with  $a$  being a generic integral (i.e.,  $g, r, t, C$ , or any other) and (anti-) symmetrization performed for all four cases  $(xp|yq)$ ,  $(ip|jq)$ ,  $(xv|yw)$ , and  $(ix|jy)$ . The symmetric combination is used in the construction of the singlet (symmetric)  $B$  or  $V$  matrix, and the anti-symmetric combination is used for the triplet (antisymmetric)  $B$  or  $V$  matrix.

$$V_{ij}^{xy(s)} + = -\tilde{r}_{pq}^{xy} \tilde{g}_{ij}^{pq} \quad (103)$$

This  $n^6$  contraction reduces to  $n^4$  if only the diagonal elements of  $B$  and  $V$  are required (e.g., for the fixed-amplitude approach). The (anti-) symmetrization procedure saves a factor of 2, because in the  $B$  and  $V$  matrices only the indices  $x \leq y$  and  $k \leq l$  need to be computed. Also, in addition to  $B$  and  $V$ , only the slice  $(ab)$  of a small number of four-index integrals need to be kept in memory at the same time, so that the memory requirements are effectively  $\mathcal{O}(N^2)$ . The matrices  $B$  and  $V$  have four indices but are usually small, because they have only geminal indices. If a diagonal approximation is used even that reduces to an  $N^2$  quantity.

For certain MP2-F12 approaches, it is necessary to solve the amplitude equations iteratively (e.g., if all amplitudes are optimized—see next section). In such cases, the four-index matrix  $C$  is used repeatedly, and it is therefore stored on disk after being computed.

For open-shell calculations, the algorithm proceeds as for the closed shell case but deviates slightly for unlike spin-pairs. Here,

the four-index integrals  $(xp|yq)$  and  $(ip|jq)$  are required for the rectangle  $p, q$ , and the intermediates  $\tilde{a}$  are not formed through (anti-)symmetrization, but through

$$\tilde{a}_{xy}^{pq} = \hat{S}_{xy} a_{xy}^{pq}, \quad (104)$$

$$\tilde{a}_{xy}^{vw} = \hat{S}_{xy} \hat{S}_{vw} a_{xy}^{vw}. \quad (105)$$

For integrals with no geminal indices,  $\tilde{a} = a$ . For spin-flipped calculations with (semi-) canonical orbitals,  $\hat{S}_{xy} a_{xy}^{pq}$  involves four-index integrals with spin-flipped indices. The necessary three-index integrals with spin-flipped indices are read from disk and contracted to form the four-index integrals at the same point as for the normal integrals. The steps where the intermediates  $\tilde{a}$  are used to build the  $B$  and  $V$  matrices proceed as for the closed-shell case.

For calculations that do not assume the EBC, contractions involving  $\{\varepsilon^{-1}\}_{klab}^{ijcd}$  are required to form  $\tilde{V}$  [eq. (34)] and  $\tilde{B}$  [eq. (39)] (or alternatively in the iterative solution of the amplitude equations 36). If the orbitals  $i, j$  are (semi-) canonical, contractions are straightforward, for example,

$$\tilde{V}_{ij}^{xy(s)} = -\tilde{C}_{ab}^{xy} g_{ij}^{ab} / (\varepsilon_a + \varepsilon_b - \varepsilon_i - \varepsilon_j) \quad (106)$$

Therefore, the four-index quantities for these contractions are always formed in the (semi-) canonical basis and subsequently transformed back to ROHF or localized orbitals if required.

In the case of parallel runs, several three-index quantities are contracted in parallel to give a four-index quantity. The resulting four-index quantities are contracted with multiple threads to give the final contribution to, for example, the  $V$  matrix. This leads to a speed-up of about 4–6 when eight threads are used—the difference to an ideal speed-up (of 8) can be traced back to the I/O of the three-index quantities, which cannot be parallelized.

### Solving for the Amplitudes

For the fixed-amplitude MP2-F12 approach, the second-order energy obtained when optimizing the amplitudes  $t_{ab}^{ij}$  in the presence of a fixed geminal contribution is computed by evaluating the Hylleraas functional, eq. (41). Having computed the matrix contributions  $T - E$ ,  $CC/\varepsilon$ ,  $-P + Q$ ,  $X$ ,  $V$  and  $Cg/\varepsilon$  using the semi-direct algorithm, these are read from disk and combined to generate the F12 contributions to the MP2 pair energies. Depending on the choice of keywords, energies for both approximations A and B are computed.

The amplitude equations for the fully optimized MP2-F12 approach eq. (36) are solved efficiently using the iterative linear equation solver routines in RICC2, where the system of equations  $s = Ac$  are solved in a reduced space of trial solution vectors  $c_1 \dots c_n$ . The initial trial solution vector is  $c_{vw}^{ij} = B^{-1,xy} \tilde{V}_{xy}^{ij}$ , and in each subsequent iteration, an additional vector is generated from  $B^{-1,xy} R_{vw}^{ij}$ . The inversion of the  $B$  matrix scales as  $O^6$ , as do the majority of the contractions when computing the residual  $R_{xy}^{ij}$ . The contractions involving the  $C$  matrix are performed in the (semi-) canonical basis using the diagonal  $\varepsilon$  and scale as  $O^4 V^2$ . The scheme for these contractions closely follows that of the semidirect algorithm in that the contraction indices  $a, b$  are slowest and only a batch ( $ab$ ) of the integrals  $C_{ab}^{xy}$  are held in memory at a given time so that

the memory requirements scale as  $O^2$ . However, as the matrix  $C$  is required many times (typically 15 iterations), rather than rebuilding  $C$  each time from the three-index quantities, it is read from disk, requiring  $O^2 V^2$  disk storage.

### Example Calculations

We have selected a few medium-sized molecules to give examples of MP2-F12 calculations that can be performed with the TURBOMOLE program package. Our selection includes drugs of various molecular size such as leflunomide, prednisone, and methotrexate, as well as technically interesting molecules such as ethylenedioxytetrathiafulvalene (EDO-TTF) and a cluster model for the adsorption of methanol on the H-ZSM-5 zeolite.

All of the calculations were performed in the basis sets cc-pVXZ-F12 with  $X = D, T$ , and  $Q$  (optimized by Peterson et al. for F12 calculations, see Ref. 4) as well as in the usual augmented correlation-consistent basis sets aug-cc-pVXZ with  $X = D, T, Q$ , and 5. A number of standard MP2 calculations were performed in the aug-cc-pV6Z basis, but no MP2-F12 calculations were performed in this basis (for the aug-cc-pV6Z basis, the auxiliary basis sets needed in a MP2-F12 calculation are not available). For MP2-F12 calculations in the double-zeta sets (cc-pVDZ-F12 and aug-cc-pVDZ), the aug-cc-pwCVTZ cbas of Ref. 40 was used for the (robust) fitting techniques for the F12 integrals and the usual MP2 electron-repulsion integrals. Accordingly, for the triple-zeta sets (cc-pVTZ-F12 and aug-cc-pVTZ), the aug-cc-pwCVQZ cbas was used, and so on.

As CABS, we used the OptRI basis sets of Yousaf and Peterson.<sup>5,6</sup> As jkbas needed for the Coulomb and exchange matrices of the Fock matrix, we used the aug-cc-pV(X+1)Z jkbas basis of Weigend<sup>41</sup> both for the cc-pVXZ-F12 as well as for the aug-cc-pVXZ orbital basis sets with  $X = D, T$ , and  $Q$ . For the aug-cc-pV5Z orbital basis, however, Weigend's aug-cc-pV5Z jkbas basis was used. All complementary auxiliary basis sets were orthogonalized using the default singular-value decomposition method with the threshold of 1.0d-08. For example, in the calculation on the molecule leflunomide in the aug-cc-cc-pV5Z basis, 74 linearly dependent CABS functions out of 3020 (ca. 2.5%) were removed by this procedure.

Finally, it is important to notice that the conventional MP2 correlation energies reported in this section were obtained using the large aug-cc-pwCV(X+1)Z cbas auxiliary basis sets mentioned above. If such conventional MP2 energies would have been computed in separate calculations (without F12 contributions), one would have used a (much) smaller auxiliary cbas basis. Hence, the conventional MP2 energies reported here are slightly different from what one would obtain in a standard calculation with TURBOMOLE. An exception are the MP2/aug-cc-pV6Z results. These were obtained using the usual aug-cc-pV6Z cbas.

### Leflunomide

Leflunomide is a pyrimidine-synthesis inhibitor belonging to the class of disease-modifying antirheumatic drugs. We have chosen

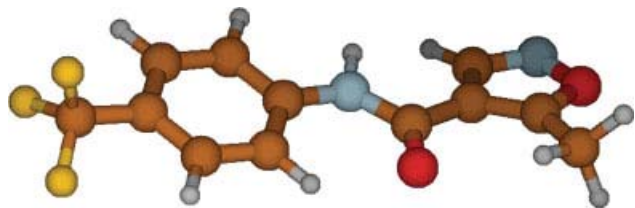


**Figure 1.** Frozen-core MP2/aug-cc-pVTZ-optimized geometry of leflunomide. The corresponding fc-MP2/aug-cc-pVTZ energy is  $-1020.5135 E_h$ .

this small molecule because it contains all atoms of the set {H, C, N, O, F} as well as an aromatic six-ring and a peptide bond as two typical molecular building blocks.

We have optimized the equilibrium geometry at the frozen-core MP2/aug-cc-pVTZ level. For the purpose of benchmarking and mutual comparison of various codes, the Cartesian coordinates of the MP2/aug-cc-pVTZ-optimized geometry are given in full detail (in atomic units) in the Supporting Information. Our optimized equilibrium geometry (Fig. 1) agrees well with the experimental X-ray structure<sup>42</sup> as well as with the geometries found in earlier theoretical studies.<sup>43</sup>

Table 4 shows the Hartree–Fock energy, the conventional MP2 correlation energy, the F12/B-*sp* correction from explicitly correlated theory, and the energy correction due to CABS singles for a series of basis sets. All of these energy contributions add up to the total energy, which is also given in Table 4. All of the calculations were performed for the MP2/aug-cc-pVTZ-optimized geometry, which was kept fixed. The aug-cc-pV6Z basis yields the lowest Hartree–Fock energy ( $-1017.0278 E_h$ ), which is expected to be close to the Hartree–Fock basis set limit. Adding the CABS singles energy correction to the aug-cc-pV5Z Hartree–Fock energy provides an energy close to this limit ( $-1017.0267 E_h$ ). The F12 correction was obtained from an MP2-F12/B-*sp* calculation, that is, using ansatz 2, approximation B, fixed amplitudes, and the [F + K] approximation. In such an MP2-F12/B-*sp* calculation, the corresponding energy for approximation A is also computed as an intermediate result, and here and in the following, we adopt the approach of Ref. 32 to estimate the MP2 basis set limit. Accordingly, we estimate the basis set limit by adding 60% of the MP2-F12/A-*sp*

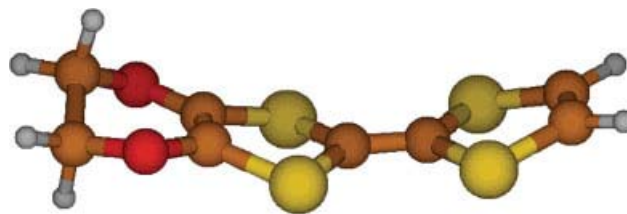


**Figure 2.** Frozen-core MP2/aug-cc-pV(T + d)Z-optimized geometry of ethylenedioxytetrafulvalene (EDO-TTF). The corresponding fc-MP2/aug-cc-pV(T + d)Z energy is  $-2048.8882 E_h$ .

energy to 40% of the MP2-F12/B-*sp* energy. For the largest basis set (aug-cc-pV5Z), we thus obtain the frozen-core second-order energy of  $E^{(2)} = -3.9615(20) E_h$ , where the error bar (to be interpreted as 95% confidence limit,  $-3.9615(20) \equiv -3.9615 \pm 0.0020$ ) has been obtained as the difference between the estimated limit and the MP2-F12/B-*sp*/aug-cc-pV5Z second-order energy. Hence, our best estimate for the basis set limit of the total (frozen-core) MP2 energy of leflunomide is  $E_{MP2} = -1020.989(2) E_h$ . Our total MP2-F12/B-*sp*/aug-cc-pV5Z energy corresponds to 99.9997% of this value, but rather than comparing total energies, it is more interesting to look at the second-order correlation energies, as is done in Table 5.

In the aug-cc-pV5Z basis, with more than 3000 contracted Gaussian basis functions, about 97.6% of the valence-shell MP2 correlation energy is obtained. Remarkably, all of the MP2-F12 calculations, even in the small double-zeta basis sets (cc-pVDZ-F12 and aug-cc-pVDZ) yield a more accurate correlation energy. When adopting a basis set limit of  $E^{(2)} = -3.9615(20) E_h$ , we observe that the correlation energy is slightly overestimated in magnitude in all of the MP2-F12/A calculations while the MP2-F12/B results are slightly smaller in magnitude. Table 5 also shows that the two-point  $X^{-3}$  extrapolation of Helgaker et al. provides excellent estimates of the basis set limit of the valence-shell MP2 correlation energy.<sup>44</sup> The (TQ), (Q5), and (56) extrapolations yield 99.4, 99.87, and 99.95%, respectively. Nevertheless, the correlation energies obtained at the MP2-F12/cc-pVTZ-F12 and MP2-F12/cc-pVQZ-F12 levels are more accurate (and more economical from a computational point of view) than these (TQ), (Q5), and (56) extrapolations.

**Table 4.** Frozen-Core Second-Order Correlation Energy (in  $E_h$ ) of Leflunomide.<sup>a</sup>

Basis	Size	Hartree–Fock	MP2	F12/B- <i>sp</i> <sup>b</sup>	$E_{CABS}$ <sup>c</sup>	Total
cc-pVDZ-F12	651	-1016.906603	-3.237780	-0.672685	-0.057063	-1020.874130
cc-pVTZ-F12	1169	-1017.007601	-3.648331	-0.301658	-0.007803	-1020.965392
cc-pVQZ-F12	1959	-1017.025846	-3.804481	-0.155646	-0.000812	-1020.986785
aug-cc-pVDZ	518	-1016.706532	-2.950163	-0.932458	-0.120568	-1020.709721
aug-cc-pVTZ	1081	-1016.949345	-3.564402	-0.366962	-0.017845	-1020.898553
aug-cc-pVQZ	1934	-1017.011610	-3.781262	-0.171607	-0.003153	-1020.967632
aug-cc-pV5Z	3133	-1017.026113	-3.866734	-0.092296	-0.000600	-1020.985743
aug-cc-pV6Z	4734	-1017.027792	-3.905763			-1020.933554

<sup>a</sup>At the frozen-core MP2/aug-cc-pVTZ-optimized geometry (cf. Fig. 1).

<sup>b</sup>Fixed amplitudes MP2-F12/B result.

<sup>c</sup>CABS singles contribution.

**Table 5.** Frozen-Core Second-Order Correlation Energy (in  $E_h$  and in %) of Leflunomide.<sup>a</sup>

Basis	Size	MP2	(%) <sup>b</sup>	MP2-F12/A- <i>sp</i> <sup>c</sup>	(%) <sup>b</sup>	MP2-F12/B- <i>sp</i> <sup>d</sup>	(%) <sup>b</sup>
cc-pVDZ-F12	651	-3.237780	(81.7)	-4.011357	(101.3)	-3.910465	(98.7)
cc-pVTZ-F12	1169	-3.648331	(92.1)	-3.978474	(100.4)	-3.949989	(99.7)
cc-pVQZ-F12	1959	-3.804481	(96.0)	-3.969558	(100.2)	-3.960128	(100.0)
aug-cc-pVDZ	518	-2.950163	(74.5)	-4.006485	(101.1)	-3.882621	(98.0)
aug-cc-pVTZ	1081	-3.564402	(90.0)	-3.966986	(100.1)	-3.931364	(99.2)
aug-cc-pVQZ	1934	-3.781262	(95.5)	-3.963171	(100.0)	-3.952869	(99.8)
aug-cc-pV5Z	3133	-3.866734	(97.6)	-3.963080	(100.0)	-3.959030	(99.9)
aug-cc-pV6Z	4734	-3.905763	(98.6)				
aug-cc-pV(DT)Z <sup>e</sup>		-3.823029	(96.5)				
aug-cc-pV(TQ)Z <sup>e</sup>		-3.939511	(99.4)				
aug-cc-pV(Q5)Z <sup>e</sup>		-3.956410	(99.9)				
aug-cc-pV(56)Z <sup>e</sup>		-3.959374	(99.9)				

<sup>a</sup>At the frozen-core MP2/aug-cc-pVTZ-optimized geometry (cf. Fig. 1).

<sup>b</sup>Percentage of the estimated basis set limit of  $E^{(2)} = -3.9615(20) E_h$ .

<sup>c</sup>Fixed amplitudes MP2-F12/A result.

<sup>d</sup>Fixed amplitudes MP2-F12/B result.

<sup>e</sup>Two-point  $X^{-3}$  extrapolation.

### EDO-TTF

Ethylenedioxy-tetrathiafulvalene (EDO-TTF) is a tetrathiafulvalene derivative with one ethylenedioxy group (cf. Fig. 2). Because this molecule contains four sulfur atoms in addition to the first-row elements, and because of its small size, we have selected it to demonstrate the performance of our MP2-F12 implementation in TURBOMOLE. We have optimized the equilibrium geometry at the frozen-core MP2/aug-cc-pV(T + d)Z level. The bent equilibrium geometry (cf. Fig. 2) is similar to the geometries found in previous work (cf. Ref. 45 and references therein). The Cartesian coordinates of the MP2/aug-cc-pV(T + d)Z-optimized geometry are given in full detail (in atomic units) in the Supporting Information. Table 6 shows the Hartree–Fock energy, the conventional MP2 correlation energy, the F12/B-*sp* correction from explicitly correlated theory, and the energy correction due to CABS singles for a series of basis sets.

As for leflunomide in the previous section, we estimate the MP2 basis set limit from adding 60% of the MP2-F12/A-*sp* energy to 40% of the MP2-F12/B-*sp* energy obtained in the aug-cc-pV(5 + d)Z

basis (Table 7). This yields  $E^{(2)} = -2.758(2) E_h$ , and we estimate the total (frozen-core) MP2 energy of EDO-TTF as  $E_{MP2} = -2049.221(2) E_h$ . Table 7 shows the percentage of the correlation energy recovered at the various levels of calculation. Despite the four sulfur atoms in this molecule, the percentages are almost identical to those obtained for leflunomide in comparable basis sets.

All of our MP2-F12 calculations in the cc-pVXZ-F12 and aug-cc-pVXZ basis sets were performed using the Slater-type geminals optimized by Peterson et al., that is, using the exponents 0.9, 1.0, and 1.1  $a_0^{-1}$  for the basis sets cc-pVDZ-F12, cc-pVTZ-F12, and cc-pVQZ-F12, and the exponents 1.1, 1.2, 1.4, and 1.4 for the basis sets aug-cc-pVXZ ( $X = D, T, Q, 5$ ), respectively.<sup>4</sup> For the molecule EDO-TTF, the dependence on the geminal exponent for the basis sets cc-pVDZ-F12, cc-pVTZ-F12, and cc-pVQZ-F12 is shown in Figure 3. Indeed, the minima of the three curves are very close to the recommended values. For EDO-TTF, we find optimal exponents of 0.92, 1.03, and 1.07  $a_0^{-1}$  for the three correlation-consistent F12 basis sets.

**Table 6.** Frozen-Core Second-Order Correlation Energy (in  $E_h$ ) of EDO-TTF.<sup>a</sup>

Basis	Size	Hartree–Fock	MP2	F12/B- <i>sp</i> <sup>b</sup>	$E_{CABS}$ <sup>c</sup>	Total
cc-pVDZ-F12	510	-2046.378756	-2.213937	-0.508065	-0.044595	-2049.145353
cc-pVTZ-F12	886	-2046.450219	-2.523995	-0.225297	-0.005631	-2049.205143
cc-pVQZ-F12	1458	-2046.461306	-2.639571	-0.117351	-0.000713	-2049.218941
aug-cc-pV(D + d)Z	412	-2046.254175	-2.052546	-0.643320	-0.092560	-2049.042600
aug-cc-pV(T + d)Z	818	-2046.413443	-2.474962	-0.261247	-0.013749	-2049.163401
aug-cc-pV(Q + d)Z	1432	-2046.453085	-2.626865	-0.123862	-0.002962	-2049.206774
aug-cc-pV(5 + d)Z	2295	-2046.461223	-2.688964	-0.067550	-0.000869	-2049.218607
aug-cc-pV(6 + d)Z	3444	-2046.462708	-2.717357			-2049.180066

<sup>a</sup>At the frozen-core MP2/aug-cc-pV(T + d)Z-optimized geometry (cf. Fig. 2).

<sup>b</sup>Fixed amplitudes MP2-F12/B result.

<sup>c</sup>CABS singles contribution.

**Table 7.** Frozen-Core Second-Order Correlation Energy (in  $E_h$  and in %) of EDO-TTF.<sup>a</sup>

Basis	Size	MP2	(%) <sup>b</sup>	MP2-F12/A- <i>sp</i> <sup>c</sup>	(%) <sup>b</sup>	MP2-F12/B- <i>sp</i> <sup>d</sup>	(%) <sup>b</sup>
cc-pVDZ-F12	510	-2.213937	(80.3)	-2.795765	(101.4)	-2.722003	(98.7)
cc-pVTZ-F12	886	-2.523995	(91.5)	-2.771442	(100.5)	-2.749293	(99.7)
cc-pVQZ-F12	1458	-2.639571	(95.7)	-2.764805	(100.2)	-2.756922	(99.9)
aug-cc-pV(D + d)Z	412	-2.052546	(74.4)	-2.774850	(100.6)	-2.695866	(97.7)
aug-cc-pV(T + d)Z	818	-2.474962	(89.7)	-2.760648	(100.1)	-2.736209	(99.2)
aug-cc-pV(Q + d)Z	1432	-2.626865	(95.2)	-2.758482	(100.0)	-2.750728	(99.7)
aug-cc-pV(5 + d)Z	2295	-2.688964	(97.5)	-2.759745	(100.0)	-2.756515	(99.9)
aug-cc-pV(6 + d)Z	3444	-2.717357	(98.5)				
aug-cc-pV(DT + d)Z <sup>e</sup>		-2.652821	(96.2)				
aug-cc-pV(TQ + d)Z <sup>e</sup>		-2.737713	(99.2)				
aug-cc-pV(Q5 + d)Z <sup>e</sup>		-2.754117	(99.8)				
aug-cc-pV(56 + d)Z <sup>e</sup>		-2.756358	(99.9)				

<sup>a</sup>At the frozen-core MP2/aug-cc-pVTZ-optimized geometry (cf. Fig. 2).

<sup>b</sup>Percentage of the estimated basis set limit of  $E^{(2)} = -2.758(2) E_h$ .

<sup>c</sup>Fixed amplitudes MP2-F12/A result.

<sup>d</sup>Fixed amplitudes MP2-F12/B result.

<sup>e</sup>Two-point  $X^{-3}$  extrapolation.

### Zeolite H-ZSM-5 Cluster Model

The explicitly correlated R12 and F12 methods have proven particularly useful for the calculation of small interaction energies. Early applications include the very weakly bound benzene...Ne and benzene...Ar van der Waals complexes<sup>46</sup> and the hydrogen-bonded H<sub>2</sub>O and HF clusters.<sup>47–49</sup> More recently, the interaction of Ar with *n*-propanol<sup>50</sup> and various 2-pyridone... (fluoro)benzene complexes were studied.<sup>14,51–53</sup>

In the present work, we have chosen the interaction of a methanol molecule with a cluster model for zeolite H-ZSM-5 as an example calculation. This model was taken from the work of Svelle et al.,<sup>20</sup> in which it was denoted as “4T” cluster model. We optimized this cluster model at the frozen-core MP2/aug-cc-pV(T + d)Z level and the corresponding Cartesian coordinates of the equilibrium geometry are given (in atomic units) in the Supporting Information (cf. Fig 4).

Tables 8 and 9 display the MP2 correlation energies calculated for the “4T” cluster model in absolute terms and as percentage of the estimated basis set limit of  $E^{(2)} = -2.128(1) E_h$ , respectively. The total energy is estimated at  $E_{\text{MP2}} = -1532.412(1) E_h$ .

At the fixed MP2/aug-cc-pV(T + d)Z geometry, we estimate the basis set limit for the frozen-core MP2 correlation contribution to the interaction energy from the counterpoise corrected MP2-F12/A and MP2-F12/B values obtained in the aug-cc-pV5Z basis. These values are  $-13.447$  and  $-13.429 mE_h$ , respectively, leading to the final best estimate of  $\Delta E_{\Delta\text{MP2}} = -13.44(1) mE_h$ . Together with the Hartree-Fock value of  $\Delta E_{\text{Hartree-Fock}} = -22.25 mE_h$ , we arrive at  $\Delta E_{\text{MP2}} = -35.69(1) mE_h$  (93.7 kJ/mol). Note that this is the purely electronic interaction energy, including neither fragment relaxation energies nor zero-point vibrational energies nor any other corrections.

Table 10 shows how the basis set limit for the frozen-core MP2 correlation contribution to the interaction energy ( $-13.44(1) mE_h$ ) is approached as a function of the basis set, at the standard MP2 as well as at the MP2-F12 level, with and without counterpoise corrections.

When discussing interaction energies, it is informative to consider the basis set superposition error (BSSE) and the counterpoise correction that corrects for it (cf. Ref. 54). Such counterpoise correction can be computed for the MP2-F12 method in exactly the same manner as for the standard MP2 approach, that is, by performing calculations on the fragments in the basis of the whole complex. As we only consider the *sp* ansatz with fixed F12 amplitudes here, we need not be concerned with the “geminal BSSE” due to the basis

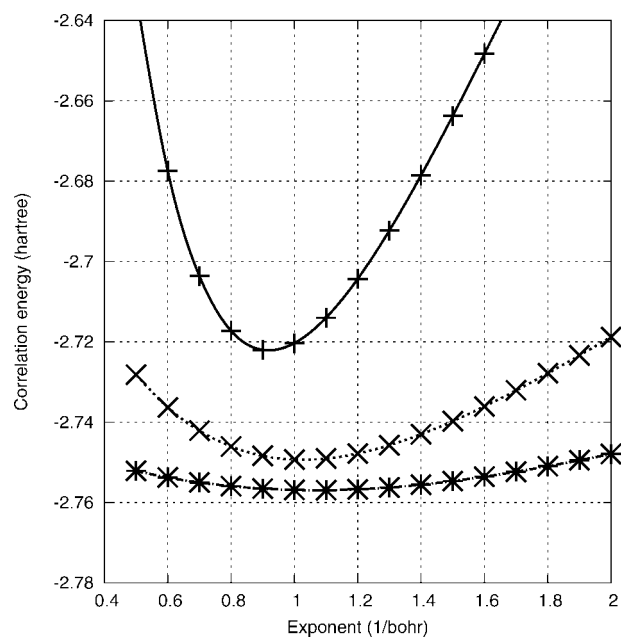


**Figure 3.** Frozen-core MP2-F12/B-*sp*/cc-pVXZ-F12 correlation energy of EDO-TTF as a function of the exponent  $\gamma$  of the Slater-type geminal. Shown are curves for the cc-pVDZ-F12 (+), cc-pVTZ-F12 (x), and cc-pVQZ-F12 (\*) basis sets.



**Table 8.** Frozen-Core Second-Order Correlation Energy (in  $E_h$ ) of the “4T” Cluster Model.<sup>a</sup>

Basis	Size	Hartree–Fock	MP2	F12/B- <i>sp</i> <sup>b</sup>	$E_{\text{CABS}}^c$	Total
cc-pVDZ-F12	471	−1530.207512	−1.707585	−0.392958	−0.037962	−1532.346022
cc-pVTZ-F12	836	−1530.271370	−1.934870	−0.185771	−0.005963	−1532.397974
cc-pVQZ-F12	1416	−1530.283290	−2.032719	−0.094065	−0.000936	−1532.411010
aug-cc-pV(D + d)Z	401	−1530.053450	−1.572188	−0.511032	−0.101311	−1532.237981
aug-cc-pV(T + d)Z	841	−1530.232249	−1.904501	−0.205513	−0.016695	−1532.358958
aug-cc-pV(Q + d)Z	1526	−1530.273793	−2.025649	−0.096758	−0.003398	−1532.399598
aug-cc-pV(5 + d)Z	2506	−1530.283074	−2.074434	−0.051886	−0.001239	−1532.410634
aug-cc-pV(6 + d)Z	3831	−1530.284810	−2.096254			−1532.381064

<sup>a</sup>At the frozen-core MP2/aug-cc-pV(T + d)Z-optimized geometry (cf. Fig. 4).<sup>b</sup>Fixed amplitudes MP2-F12/B result.<sup>c</sup>CABS singles contribution.

set superposition of geminal basis functions.<sup>55</sup> When using the *sp* ansatz, there is no such geminal BSSE.

Table 10 immediately shows that the BSSE is significant in all of the standard MP2 calculations. Even in the largest basis set (aug-cc-pV(6 + d)Z), the counterpoise correction to the correlation contribution to the interaction energy amounts to 0.47  $mE_h$ , which is about 100 times larger than the corresponding correction at the Hartree–Fock level (ca. 0.005  $mE_h$ ). Incidentally, we note that taking the average of the uncorrected (−13.84  $mE_h$ ) and corrected (−13.05  $mE_h$ ) aug-cc-pV(5 + d)Z energies gives a remarkably good estimate of the limiting value. The same average interaction energy is obtained in the aug-cc-pV(6 + d)Z basis.

Also at the MP2-F12 level the basis set superposition error is non-negligible, being of the same order of magnitude as the Hartree–Fock BSSE. However, except for the largest basis sets (cc-pVQZ-F12 and aug-cc-pV(5 + d)Z), the counterpoise correction to the MP2-F12 correlation contribution is smaller than the corresponding correction to the Hartree–Fock interaction energy

(Table 11). When including a counterpoise correction to the MP2-F12 correlation contributions, the basis set convergence is very fast. Already in the aug-cc-pV(D + d)Z and aug-cc-pV(T + d)Z basis sets, the electron correlation contributions are within 0.3 and 0.1  $mE_h$  of the basis set limit, respectively.

#### Prednisone and Methotrexate

The frozen-core MP2/aug-cc-pVDZ equilibrium structure of prednisone is shown in Figure 5 and is available from the Supporting Information. It agrees very well with the 3D structure found in the University of Alberta’s database DRUGBANK,<sup>56,57</sup> except for the orientation of the  $-\text{CH}_2\text{OH}$  group.

Table 12 shows the Hartree–Fock energy, the conventional MP2 correlation energy, the F12/B-*sp* correction from explicitly correlated theory, and the energy correction due to CABS singles for a series of basis sets. MP2-F12/A-*sp* and MP2-F12/B-*sp* correlation energies are given in Table 13. We estimate the basis set limit for the second-order energy at  $E^{(2)} = -5.197(7) E_h$ , of which already more

**Table 9.** Frozen-Core Second-Order Correlation Energy (in  $E_h$  and in %) of the “4T” Cluster Model.<sup>a</sup>

Basis	Size	MP2	(%) <sup>b</sup>	MP2-F12/A- <i>sp</i> <sup>c</sup>	(%) <sup>b</sup>	MP2-F12/B- <i>sp</i> <sup>d</sup>	(%) <sup>b</sup>
cc-pVDZ-F12	471	−1.707585	(80.3)	−2.158991	(101.5)	−2.100543	(98.7)
cc-pVTZ-F12	836	−1.934870	(90.9)	−2.138805	(100.5)	−2.120641	(99.7)
cc-pVQZ-F12	1416	−2.032719	(95.5)	−2.132798	(100.2)	−2.126784	(100.0)
aug-cc-pV(D + d)Z	401	−1.572188	(73.9)	−2.149952	(101.0)	−2.083220	(97.9)
aug-cc-pV(T + d)Z	841	−1.904501	(89.5)	−2.129371	(100.1)	−2.110014	(99.2)
aug-cc-pV(Q + d)Z	1526	−2.025649	(95.2)	−2.128141	(100.0)	−2.122407	(99.8)
aug-cc-pV(5 + d)Z	2506	−2.074434	(97.5)	−2.128597	(100.0)	−2.126320	(99.9)
aug-cc-pV(6 + d)Z	3831	−2.096254	(98.5)				
aug-cc-pV(DT + d)Z <sup>e</sup>		−2.044422	(96.1)				
aug-cc-pV(TQ + d)Z <sup>e</sup>		−2.114054	(99.4)				
aug-cc-pV(Q5 + d)Z <sup>e</sup>		−2.125618	(99.9)				
aug-cc-pV(56 + d)Z <sup>e</sup>		−2.126227	(99.9)				

<sup>a</sup>At the frozen-core MP2/aug-cc-pVTZ-optimized geometry (cf. Fig. 4).<sup>b</sup>Percentage of the estimated basis set limit of  $E^{(2)} = -2.128(1) E_h$ .<sup>c</sup>Fixed amplitudes MP2-F12/A result.<sup>d</sup>Fixed amplitudes MP2-F12/B result.<sup>e</sup>Two-point  $X^{-3}$  extrapolation.

**Table 10.** Hartree–Fock and Frozen-Core Second-Order Interaction Energies (in  $mE_h$ ) for Methanol Adsorbed on the Zeolite H-ZSM-5 Cluster Model.<sup>a</sup>

Basis	Size	Hartree–Fock			MP2 <sup>b</sup>			MP2-F12/B- <i>sp</i> <sup>c</sup>		
		$\Delta E^d$	CP <sup>e</sup>	$\Delta E_{CP}^f$	$\Delta E^d$	CP <sup>e</sup>	$\Delta E_{CP}^f$	$\Delta E^d$	CP <sup>e</sup>	$\Delta E_{CP}^f$
cc-pVDZ-F12	471	−23.31	1.00	−22.32	−12.51	2.89	−9.62	−13.38	0.32	−13.07
cc-pVTZ-F12	836	−22.40	0.24	−22.16	−13.88	2.00	−11.88	−13.53	0.19	−13.34
cc-pVQZ-F12	1416	−22.28	0.04	−22.24	−13.72	0.99	−12.73	−13.50	0.08	−13.42
aug-cc-pV(D + d)Z	401	−24.17	2.46	−21.71	−14.15	4.71	−9.44	−13.64	0.48	−13.16
aug-cc-pV(T + d)Z	841	−22.87	0.83	−22.05	−14.75	2.92	−11.83	−13.75	0.37	−13.38
aug-cc-pV(Q + d)Z	1526	−22.39	0.15	−22.24	−14.16	1.45	−12.71	−13.62	0.21	−13.41
aug-cc-pV(5 + d)Z	2506	−22.28	0.03	−22.25	−13.84	0.79	−13.05	−13.52	0.09	−13.43
aug-cc-pV(6 + d)Z	3831	−22.25	0.00	−22.25	−13.68	0.47	−13.21			
aug-cc-pV(DT + d)Z <sup>g</sup>							−12.83			
aug-cc-pV(TQ + d)Z <sup>g</sup>							−13.36			
aug-cc-pV(Q5 + d)Z <sup>g</sup>							−13.40			
aug-cc-pV(56 + d)Z <sup>g</sup>							−13.42			

<sup>a</sup>At the frozen-core MP2/aug-cc-pV(T + d)Z-optimized geometry (cf. Fig. 4).

<sup>b</sup>Correlation contribution only.

<sup>c</sup>Fixed amplitudes MP2-F12/B result; correlation contribution only.

<sup>d</sup>Interaction energy with respect to fragments that were kept fixed in the complex geometry.

<sup>e</sup>Counterpoise correction.

<sup>f</sup>Interaction energy including counterpoise correction.

<sup>g</sup>Two-point  $X^{-3}$  extrapolation.

than 99% is obtained at the MP2-F12/B-*sp*/cc-pVDZ-F12 level. The aug-cc-pV(TQ)Z and (Q5) extrapolations are comparable in quality with the MP2-F12/B-*sp*/aug-cc-pVTZ and aug-cc-pVQZ results, but note that the latter calculations are more economical.

The frozen-core MP2/aug-cc-pVDZ equilibrium structure of methotrexate is shown in Figure 6 and is available from the Supporting Information. Our structure is clearly different from the DRUGBANK 3D structure<sup>56,57</sup> as well as from other reported structures.<sup>58–60</sup> This is understandable, because we have optimized an isolated molecule and not the crystal structure of methotrexate tetrahydrate. We have found an equilibrium structure with two intramolecular hydrogen bonds (cf. Fig. 6). In a comprehensive study of the molecular conformations of methotrexate by force field techniques, 1,250 minima were found within 10 kcal/mol above the respective global minimum.<sup>60</sup> Note that the lowest-energy minimum in Kollman's force field is rather different from our structure, with only one intramolecular hydrogen bond.<sup>60</sup>

Tables 14 and 15 list the relevant Hartree–Fock, MP2, and MP2-F12 energies. We estimate the basis set limit for the second-order energy at  $E^{(2)} = -6.755(9) E_h$ , of which already about 99% is obtained at the MP2-F12/B-*sp*/cc-pVDZ-F12 level. The excellent performance of the MP2-F12/B-*sp*/cc-pVDZ-F12 level of calculation is demonstrated.

### Computation Times

All of the calculations presented in this article were performed on a heterogeneous Intel® Xeon® compute server containing X5460 3.16 GHz, E5640 2.67 GHz, and E5530 2.40 GHz processors. Table 16 reports the measured computation times (wall clock) of the calculations performed on the leflunomide molecule in the aug-cc-pVXZ basis sets. These computation times were taken from

the calculations done for Table 4, which were not performed on a dedicated processor but rather on various processor types and under normal working conditions, that is, under load. By running one particular MP2-F12 calculation simultaneously on all processors of the compute server (under load), we found that the ratio between the fastest and the slowest calculations was about 1.5 with respect to wall-clock time. Hence, the timings reported in Table 16 provide rather crude estimates of the timings that one may expect from this kind of calculations in real-life applications. Table 16 gives, however, a proper impression of the “order of magnitude” of the computation times of Hartree–Fock, conventional MP2, and explicitly correlated MP2-F12 calculations.

All Hartree–Fock calculations of the present work were carried out without any approximations (column under the header “HF”). When the cardinal number  $X$  of the basis set is increased by 1, the Hartree–Fock computation time increases roughly by a factor of 9 (note that the calculations in the aug-cc-pV5Z and aug-cc-pV6Z basis sets were run in parallel, because in terms of one process, these calculations would have taken 2 months and 1.5 years, respectively). The MP2-F12/2A\* calculations are considerably faster than the Hartree–Fock calculations, even when using just one thread. In the larger basis sets, the difference between MP2-F12/2A\* and Hartree–Fock calculations is about one order of magnitude. The MP2-F12/2B calculations take about four to five times longer than the MP2-F12/2A\* calculations, but they are still faster than their underlying Hartree–Fock calculation, except in the small aug-cc-pVDZ and aug-cc-pVTZ basis sets.

When comparing the sequential MP2-F12 calculations with those that were run in parallel using eight threads (OpenMP), we find that the speed-up amounts to about only 4–5, significantly below 8. This can be explained by the I/O involved and by the fact that the processor time in the parallel calculations may be up to about 30%

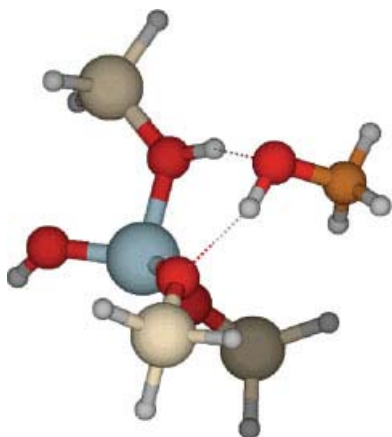
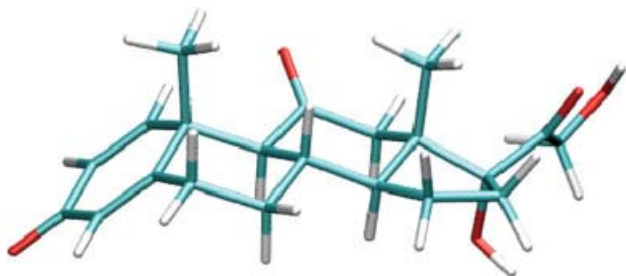


**Figure 4.** Frozen-core MP2/aug-cc-pV(T+d)Z-optimized geometry of the “4T” cluster model for zeolite H-ZSM-5 with adsorbed methanol.<sup>20</sup> The corresponding fc-MP2/aug-cc-pV(T + d)Z energy is  $-1532.1367 E_h$ .

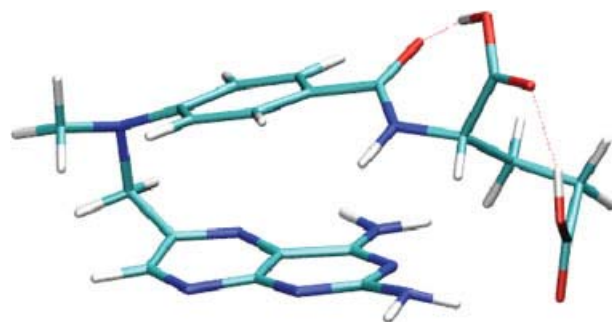
larger than in the sequential calculation (e.g., the OpenMP parallel calculation needs more core memory, and as a result, some intermediate quantities need to be re-evaluated more often than in the corresponding sequential calculation).

Table 16 furthermore provides a comparison between explicitly correlated MP2-F12 and conventional MP2 calculations. As the auxiliary basis *cbas* in the MP2-F12 calculations is larger than the one that is used in a separate conventional MP2 calculation, the table contains two columns for the two different *cbas* basis sets. The MP2 calculation with the standard *cbas* basis is the most relevant one, because this is how regular conventional MP2 calculations are performed (for the aug-cc-pV6Z basis, there exists only a standard *cbas* basis). Table 16 shows that the MP2-F12/2A\* calculations using eight threads take about six times more computation time than the conventional MP2 calculations (standard *cbas*). With only one thread, the factor is about 20.

We observe that virtually all MP2 and MP2-F12 calculations are significantly faster than the underlying Hartree–Fock calculation, which needs about 20 iterations. Hence, the Hartree–Fock calculations have been a major bottleneck in the calculations presented in this article. However, Hartree–Fock calculations can alternatively be carried out using the RIJK approximation of Weigend.<sup>41</sup> The



**Figure 5.** Frozen-core MP2/aug-cc-pVDZ-optimized geometry of prednisone. The corresponding fc-MP2/aug-cc-pVDZ energy is  $-1188.7839 E_h$ .



**Figure 6.** Frozen-core MP2/aug-cc-pVDZ-optimized geometry of methotrexate. The corresponding fc-MP2/aug-cc-pVDZ energy is  $-1585.5005 E_h$ .

timings of such calculations are also reported in Table 16, both for the standard *jkbas* and for the larger *jkbas* used in the MP2-F12 calculations. The reduction of computation time by virtue of the RIJK approximation is substantial. Using the standard *jkbas* basis, the Hartree–Fock timings are of the same order of magnitude as the MP2-F12/2A\* calculation using eight threads.

In conclusion, Table 16 shows that MP2-F12 calculations can be performed in large basis sets for sizable molecules in reasonable computation times. For leflunomide in the aug-cc-pV5Z basis (3133 basis functions), for example, a Hartree–Fock calculation using the standard RIJK approximation, followed by a MP2-F12/2A\* calculation using eight threads, takes altogether only about 54 h, that is, a little more than 2 days. A correlation energy of  $-3.9635 E_h$  (100.05% of the estimated basis set limit) is obtained in such a calculation on a molecule with 28 atoms.

Concerning basis set extrapolation techniques, we note that the correlation energy of leflunomide obtained at the extrapolated aug-cc-pV(Q5)Z level amounts to  $-3.9564 E_h$  (99.87%). The calculations required for this extrapolation add up to 44 h when the RIJK approximation is invoked in the aug-cc-pVQZ and aug-cc-pV5Z Hartree–Fock calculations, but to 70 days without this approximation. A comparably accurate correlation energy can be obtained at the MP2-F12/2B level in the aug-cc-pVTZ basis. The corresponding calculations take between 7 and 46 h (times for Hartree–Fock with RIJK plus MP2-F12/2B with eight threads versus Hartree–Fock without RIJK plus MP2-F12/2B with 1 thread). At the MP2-F12/2A\* level, the corresponding computation times are 3 and 27 h, respectively. The MP2-F12 calculations clearly outperform basis set extrapolation techniques.

## Concluding Remarks

The aim of this article was to present the details of the MP2-F12 method for ground state energies as implemented in the TURBOMOLE program. The range of utility currently affordable has been demonstrated by large-scale MP2-F12 calculations of systems with up to 55 atoms and 3652 contracted basis functions (methotrexate; 4323, 6644, and 13,618 functions in the CABS, *jkbas*, and *cbas* basis sets, respectively). The hope is expressed that this article may serve as a valuable reference for future work in the field as well as for users of the MP2-F12 implementation in TURBOMOLE.

**Table 11.** Hartree–Fock (HF) Interaction Energies (in  $mE_h$ ), Obtained with and without CABS Singles Contribution, for Methanol Adsorbed on the Zeolite H-ZSM-5 Cluster Model.<sup>a</sup>

Basis	Size	HF w/o CABS singles			HF w/CABS singles		
		$\Delta E^b$	CP <sup>c</sup>	$\Delta E_{CP}^d$	$\Delta E^b$	CP <sup>c</sup>	$\Delta E_{CP}^d$
cc-pVDZ-F12	471	−23.31	1.00	−22.32	−22.43	0.23	−22.20
cc-pVTZ-F12	836	−22.40	0.24	−22.16	−22.31	0.08	−22.23
cc-pVQZ-F12	1416	−22.28	0.04	−22.24	−22.27	0.02	−22.25
aug-cc-pV(D + d)Z	401	−24.17	2.46	−21.71	−22.82	0.79	−22.03
aug-cc-pV(T + d)Z	841	−22.87	0.83	−22.05	−22.41	0.21	−22.20
aug-cc-pV(Q + d)Z	1526	−22.39	0.15	−22.24	−22.31	0.07	−22.24
aug-cc-pV(5 + d)Z	2506	−22.28	0.03	−22.25	−22.26	0.01	−22.25
aug-cc-pV(6 + d)Z	3831	−22.25	0.00	−22.25			

<sup>a</sup>At the frozen-core MP2/aug-cc-pV(T + d)Z-optimized geometry (cf. Fig. 4).<sup>b</sup>Interaction energy with respect to fragments that were kept fixed in the complex geometry.<sup>c</sup>Counterpoise correction.<sup>d</sup>Interaction energy including counterpoise correction.**Table 12.** Frozen-Core Second-Order Correlation Energy (in  $E_h$ ) of Prednisone.<sup>a</sup>

Basis	Size	Hartree–Fock	MP2	F12/B- <i>sp</i> <sup>b</sup>	$E_{CABS}^c$	Total
cc-pVDZ-F12	1014	−1185.014786	−4.313639	−0.834380	−0.056935	−1190.219740
cc-pVTZ-F12	1846	−1185.118692	−4.811202	−0.375624	−0.009403	−1190.314920
cc-pVQZ-F12	3146	−1185.139089	−5.007141	−0.189589	−0.001141	−1190.336959
aug-cc-pVDZ	832	−1184.805928	−3.978297	−1.134315	−0.124087	−1190.042626
aug-cc-pVTZ	1794	−1185.055743	−4.735309	−0.434898	−0.020817	−1190.246767
aug-cc-pVQZ	3276	−1185.124360	−4.989929	−0.200175	−0.003674	−1190.318137
aug-cc-pV5Z	5382	−1185.139550	−5.088523			−1190.228073

<sup>a</sup>At the frozen-core MP2/aug-cc-pVDZ optimized geometry (cf. Fig. 5).<sup>b</sup>Fixed amplitudes MP2-F12/B result.<sup>c</sup>CABS singles contribution.**Table 13.** Frozen-Core Second-Order Correlation Energy (in  $E_h$  and in %) of Prednisone.<sup>a</sup>

Basis	Size	MP2	(%) <sup>b</sup>	MP2-F12/A- <i>sp</i> <sup>c</sup>	(%) <sup>b</sup>	MP2-F12/B- <i>sp</i> <sup>d</sup>	(%) <sup>b</sup>
cc-pVDZ-F12	1014	−4.313639	(83.0)	−5.267677	(101.4)	−5.148019	(99.1)
cc-pVTZ-F12	1846	−4.811202	(92.6)	−5.221831	(100.5)	−5.186825	(99.8)
cc-pVQZ-F12	3146	−5.007141	(96.3)	−5.208255	(100.2)	−5.196729	(100.0)
aug-cc-pVDZ	832	−3.978297	(76.6)	−5.252903	(101.1)	−5.112611	(98.4)
aug-cc-pVTZ	1794	−4.735309	(91.1)	−5.209878	(100.2)	−5.170207	(99.5)
aug-cc-pVQZ	3276	−4.989929	(96.0)	−5.201553	(100.1)	−5.190104	(99.9)
aug-cc-pV5Z	5382	−5.088523	(97.9)				
aug-cc-pV(DT)Z <sup>e</sup>		−5.054051	(97.2)				
aug-cc-pV(TQ)Z <sup>e</sup>		−5.175732	(99.6)				
aug-cc-pV(Q5)Z <sup>e</sup>		−5.191966	(99.9)				

<sup>a</sup>At the frozen-core MP2/aug-cc-pVTZ-optimized geometry (cf. Fig. 5).<sup>b</sup>Percentage of the estimated basis set limit of  $E^{(2)} = -5.197(7) E_h$ .<sup>c</sup>Fixed amplitudes MP2-F12/A result.<sup>d</sup>Fixed amplitudes MP2-F12/B result.<sup>e</sup>Two-point  $X^{-3}$  extrapolation.

**Table 14.** Frozen-Core Second-Order Correlation Energy (in  $E_h$ ) of methotrexate.<sup>a</sup>

Basis	Size	Hartree–Fock	MP2	F12/B- <i>sp</i> <sup>b</sup>	$E_{\text{CABS}}$ <sup>c</sup>	Total
cc-pVDZ-F12	1188	−1580.611852	−5.604259	−1.085817	−0.087707	−1587.389635
cc-pVTZ-F12	2145	−1580.762283	−6.256507	−0.484984	−0.012193	−1587.515967
cc-pVQZ-F12	3619	−1580.788748	−6.509727	−0.245154	−0.001420	−1587.545051
aug-cc-pVDZ	957	−1580.342976	−5.157446	−1.486306	−0.171340	−1587.158068
aug-cc-pVTZ	2024	−1580.677917	−6.142324	−0.575444	−0.028657	−1587.424342
aug-cc-pVQZ	3652	−1580.769575	−6.479852	−0.265566	−0.004642	−1587.519635
aug-cc-pV5Z	5951	−1580.789241	−6.611223			−1587.400463

<sup>a</sup>At the frozen-core MP2/aug-cc-pVDZ optimized geometry (cf. Fig. 6).<sup>b</sup>Fixed amplitudes MP2-F12/B result.<sup>c</sup>CABS singles contribution.**Table 15.** Frozen-Core Second-Order Correlation Energy (in  $E_h$  and in %) of Methotrexate.<sup>a</sup>

Basis	Size	MP2	(%) <sup>b</sup>	MP2-F12/A- <i>sp</i> <sup>c</sup>	(%) <sup>b</sup>	MP2-F12/B- <i>sp</i> <sup>d</sup>	(%) <sup>b</sup>
cc-pVDZ-F12	1180	−5.604259	(83.0)	−6.847109	(101.4)	−6.690075	(99.0)
cc-pVTZ-F12	2145	−6.256507	(92.6)	−6.786752	(100.5)	−6.741491	(99.8)
cc-pVQZ-F12	3619	−6.509727	(96.4)	−6.769759	(100.2)	−6.754882	(100.0)
aug-cc-pVDZ	957	−5.157446	(76.4)	−6.829593	(101.1)	−6.643752	(98.4)
aug-cc-pVTZ	2024	−6.142324	(90.9)	−6.771182	(100.2)	−6.717769	(99.5)
aug-cc-pVQZ	3652	−6.479852	(95.9)	−6.760844	(100.1)	−6.745419	(99.9)
aug-cc-pV5Z	5951	−6.611223	(97.9)				
aug-cc-pV(DT)Z <sup>e</sup>		−6.557010	(97.1)				
aug-cc-pV(TQ)Z <sup>e</sup>		−6.726156	(99.6)				
aug-cc-pV(Q5)Z <sup>e</sup>		−6.749054	(99.9)				

<sup>a</sup>At the frozen-core MP2/aug-cc-pVTZ-optimized geometry (cf. Fig. 6).<sup>b</sup>Percentage of the estimated basis set limit of  $E^{(2)} = -6.755(9) E_h$ .<sup>c</sup>Fixed amplitudes MP2-F12/A result.<sup>d</sup>Fixed amplitudes MP2-F12/B result.<sup>e</sup>Two-point  $X^{-3}$  extrapolation.**Table 16.** Computation Times (Wall-Clock Time in Minutes)<sup>a</sup> of Various Hartree–Fock (20 iterations), MP2-F12/2B-*sp* [F + K], and MP2-F12/2A\*-*sp* [T + V] calculations on leflunomide;  $n$  is the number of threads.

Basis	HF	HF RIJK <sup>d</sup>	HF RIJK <sup>e</sup>	MP2 <sup>b</sup>	MP2 <sup>c</sup>	F12/2B $n = 1$	F12/2B $n = 8$	F12/2A* $n = 1$	F12/2A* $n = 8$
aug-cc-pVDZ	118	40	26	2	5	432	95	95	20
aug-cc-pVTZ	1211	96	147	13	28	1549	344	385	83
aug-cc-pVQZ	10086	367	626	70	129	6054	1374	1609	419
aug-cc-pV5Z	90431 <sup>f</sup>	1938	2941	258	398	19011	3719	4541	1296
aug-cc-pV6Z	817018 <sup>g</sup>			993					

<sup>a</sup>Measured on Intel® Xeon® X5460 3.16 GHz, E5640 2.67 GHz, and E5530 2.40 GHz.<sup>b</sup>Using the standard *cbas* basis.<sup>c</sup>Using the same *cbas* basis as used in the MP2-F12/2A\* and -2B calculations.<sup>d</sup>Using the standard *jkbas* basis.<sup>e</sup>Using the same *jkbas* basis as used in the MP2-F12/2A\* and -2B calculations.<sup>f</sup>Six times the time measured in a parallel run with six processes.<sup>g</sup>Eight times the time measured in a parallel run with eight processes.

## References

1. Klopper, W.; Bachorz, R. A.; Hättig, C.; Tew, D. P. *Theor Chem Acc* 2010, 126, 289.
2. Klopper, W.; Ruscic, B.; Tew, D. P.; Bischoff, F. A.; Wolfsegger, S. *Chem Phys* 2009, 356, 14.
3. Bischoff, F. A.; Wolfsegger, S.; Tew, D. P.; Klopper, W. *Mol Phys* 2009, 107, 963.
4. Peterson, K. A.; Adler, T. B.; Werner, H.-J. *J Chem Phys* 2008, 128, 084102.
5. Yousaf, K. E.; Peterson, K. A. *J Chem Phys* 2008, 129, 184108.
6. Yousaf, K. E.; Peterson, K. A. *Chem Phys Lett* 2009, 476, 303.
7. Hill, J. G.; Peterson, K. A. *Phys Chem Chem Phys* 2010, 12, 10460.
8. Hill, J. G.; Mazumder, S.; Peterson, K. A. *J Chem Phys* 2010, 132, 054108.
9. Hill, J. G.; Peterson, K. A.; Knizia, G.; Werner, H.-J. *J Chem Phys* 2009, 131, 194105.
10. Helgaker, T.; Klopper, W.; Tew, D. P. *Mol Phys* 2008, 106, 2107.
11. Tew, D. P.; Klopper, W.; Helgaker, T. *J Comput Chem* 2007, 28, 1307.
12. Hättig, C.; Tew, D. P.; Köhn, A. *J Chem Phys* 2010, 132, 231102.
13. Grimme, S. *J Chem Phys* 2003, 118, 9095.
14. Bachorz, R. A.; Bischoff, F. A.; Höfener, S.; Klopper, W.; Ottinger, P.; Leist, R.; Frey, J. A.; Leutwyler, S. *Phys Chem Chem Phys* 2008, 10, 2758.
15. Jung, T.; Beckhaus, R.; Klüner, T.; Höfener, S.; Klopper, W. *J Chem Theor Comput* 2009, 5, 2044.
16. Mata, R. A.; Werner, H.-J.; Thiel, S.; Thiel, W. *J Chem Phys* 2008, 128, 025104.
17. Vogiatzis, K. D.; Barnes, E. C.; Klopper, W. *Chem Phys Lett* 2011, 503, 157.
18. TURBOMOLE V6.3, 2011; Available at: <http://www.turbomole.com>.
19. Ahlrichs, R.; Bär, M.; Häser, M.; Horn, H.; Kölmel, C. *Chem Phys Lett* 1989, 162, 165.
20. Svelle, S.; Tuma, C.; Rozanska, X.; Kerber, T.; Sauer, J. *J Am Chem Soc* 2009, 131, 816.
21. Bischoff, F. A.; Höfener, S.; Glöß, A.; Klopper, W. *Theor Chem Acc* 2008, 121, 11.
22. Burow, A. M.; Sierka, M.; Döbler, J.; Sauer, J. *J Chem Phys* 2009, 130, 174710.
23. Tew, D. P.; Klopper, W. *J Chem Phys* 2005, 123, 074101.
24. Adler, T. B.; Knizia, G.; Werner, H.-J. *J Chem Phys* 2007, 127, 221106.
25. Knizia, G.; Werner, H.-J. *J Chem Phys* 2008, 128, 154103.
26. Weigend, F.; Häser, M. *Theor Chem Acc* 1997, 97, 331.
27. Weigend, F.; Köhn, A.; Hättig, C. *J Chem Phys* 2002, 116, 3175.
28. Kutzelnigg, W.; Klopper, W. *J Chem Phys* 1991, 94, 1985.
29. Vahtras, O.; Almlöf, J.; Feyereisen, M. W. *Chem Phys Lett* 1993, 213, 514.
30. Manby, F. R. *J Chem Phys* 2003, 119, 4607.
31. Glöß, A. Entwicklung und Implementierung schneller MP2-R12-Methoden, Universität Karlsruhe (TH), Germany, 2008; URN (NBN): urn:nbn:de:swb:90-93603.
32. Samson, C. C. M.; Klopper, W. *Mol Phys* 2004, 102, 2499.
33. Klopper, W.; Samson, C. C. M. *J Chem Phys* 2002, 116, 6397.
34. Kedžuch, S.; Milko, M.; Noga, J. *Int J Quantum Chem* 2005, 105, 929.
35. Werner, H.-J.; Adler, T. B.; Manby, F. R. *J Chem Phys* 2007, 126, 164102.
36. Klopper, W.; Kutzelnigg, W. *Chem Phys Lett* 1987, 134, 17.
37. Ten-no, S. *J Chem Phys* 2004, 121, 117.
38. Boys, S. F. In *Quantum Theory of Atoms, Molecules and the Solid State*; Löwdin, P.-O., Ed.; Academic Press: New York, 1966; p. 253.
39. Pipek, J.; Mezey, P. G. *J Chem Phys* 1989, 90, 4916.
40. Hättig, C. *Phys Chem Chem Phys* 2005, 7, 59.
41. Weigend, F. *J Comput Chem* 2008, 29, 167.
42. Vega, D.; Petragalli, A.; Fernández, D.; Ellena, J. A. *J Pharm Sci* 2008, 95, 1075.
43. Panek, J. J.; Jezierska, A.; Mierzwicki, K.; Latajka, Z.; Kroll, A. *J Chem Inf Model* 2005, 45, 39.
44. Helgaker, T.; Klopper, W.; Koch, H.; Noga, J. *J Chem Phys* 1997, 106, 9639.
45. Linker, G.-J.; van Loosdrecht, P. H. M.; van Duijnen, P.; Broer, R. *Chem Phys Lett* 2010, 487, 220.
46. Klopper, W.; Lüthi, H. P.; Brupbacher, T.; Bauder, A. *J Chem Phys* 1994, 101, 9747.
47. Klopper, W.; Schütz, M.; Lüthi, H. P.; Leutwyler, S. *J Chem Phys* 1995, 103, 1085.
48. Schütz, M.; Klopper, W.; Lüthi, H. P.; Leutwyler, S. *J Chem Phys* 1995, 103, 6114.
49. Klopper, W.; Quack, M.; Suhm, M. A. *Mol Phys* 1998, 94, 105.
50. Lee, J. J.; Höfener, S.; Klopper, W.; Wassermann, T. N.; Suhm, M. A. *J Phys Chem C* 2009, 113, 10929.
51. Leist, R.; Frey, J. A.; Ottinger, P.; Frey, H.-M.; Leutwyler, S.; Bachorz, R. A.; Klopper, W. *Angew Chem Int Ed Engl* 2007, 46, 7449.
52. Ottinger, P.; Pfaffen, C.; Leist, R.; Leutwyler, S.; Bachorz, R. A.; Klopper, W. *J Phys Chem B* 2009, 113, 2937.
53. Pfaffen, C.; Frey, H.-M.; Ottinger, P.; Leutwyler, S.; Bachorz, R. A.; Klopper, W. *Phys Chem Chem Phys* 2010, 12, 8208.
54. van Duijneveldt, F. B.; van Duijneveldt-van de Rijdt, J. G. C. M.; van Lenthe, J. *Chem Rev* 1994, 94, 1873.
55. Tew, D. P.; Klopper, W. *J Chem Phys* 2006, 125, 094302.
56. Wishart, D. S.; Knox, C.; Guo, A. C.; Cheng, D.; Shrivastava, S.; Tzur, D.; Gautam, B.; Hassanali, M. *Nucl Acids Res* 2008, 36, D901.
57. Wishart, D. S.; Knox, C.; Guo, A. C.; Shrivastava, S.; Hassanali, M.; Stothard, P.; Chang, Z.; Woolsey, J. *Nucl Acids Res* 2008, 34, D668.
58. Sutton, P. A.; Cody, V.; Smith, G. D. *J Am Chem Soc* 1986, 108, 4155.
59. Mastropaolo, D.; Camerman, A.; Camerman, N. *J Med Chem* 2001, 44, 269.
60. Tosi, C.; Fusco, R.; Caccianotti, L. *J Mol Struct (Theochem)* 1989, 183, 361.